Maxwell's Equations and QED: Which is Fact and Which is Fiction

Randell L. Mills, BlackLight Power, Inc., 493 Old Trenton Road, Cranbury, NJ 08512

(609)490-1090, rmills@blacklightpower.com, www.blacklightpower.com

Abstract

The claim that quantum electrodynamics (QED) is the most successful theory in history is critically evaluated. The Dirac equation was postulated in 1926 as a means to remedy the nonrelativistic nature of the Schrödinger equation to provide the missed fourth quantum number. The positive as well as negative square root terms provided an argument for the existence of negative energy states of the vacuum, virtual particles, and corresponding so-called quantum electrodynamics (QED) computer algorithms for calculating unexpected observables such as the Lamb shift and the anomalous magnetic moment of the electron. Dirac's original attempt to solve the bound electron physically with stability with respect to radiation according to Maxwell's equations with the further constraints that it was relativistically invariant and gives rise to electron spin is achievable using a classical approach. Starting with the same essential physics as Bohr, Schrödinger, and Dirac of e^- moving in the Coulombic field of the proton and the wave equation as an equation of motion rather than energy after Schrödinger, advancements in the understanding of the stability of the bound electron to radiation are applied to solve for the exact nature of the electron. Rather than using the postulated Schrödinger boundary condition: "$\Psi \to 0$ as $r \to \infty$", which leads to a purely mathematical model of the electron, the constraint is based on experimental observation. Using Maxwell's equations, *the classical wave equation is solved with the constraint that the bound* $n = 1$*-state electron cannot radiate energy*. Although it is well known that an accelerated *point* particle radiates, an *extended distribution*

modeled as a superposition of accelerating charges does not have to radiate. A simple invariant physical model arises naturally wherein the predicted results are extremely straightforward and internally consistent requiring minimal mathematics as in the case of the most famous equations of Newton, Maxwell, Einstein, de Broglie, and Planck on which the model is based. No new physics is needed; only the known physical laws based on direct observation are used. Rather than invoking untestable "flights of fantasy", the results of QED such as the anomalous magnetic moment of the electron, the Lamb Shift, the fine structure and hyperfine structure of the hydrogen atom, and the hyperfine structure intervals of positronium and muonium can be solved exactly from Maxwell's equations to the limit possible based on experimental measurements which confirms QED's illegitimacy as representative of reality.

Key Words: QED, Maxwell's equations, Lamb Shift, fine structure and hyperfine structure of the hydrogen atom, hyperfine structure intervals of positronium and muonium

Contents

I. Introduction

The hydrogen atom is the only real problem for which the Schrödinger equation can be solved without approximations; however, it only provides three quantum numbers—not four. Furthermore, the Schrödinger equation is not accurate at all. It is nonrelativistic, and there are major differences between predicted and experimental ionization energies as Z increases, and inescapable disagreements between observation and predictions arise from the later postulated Dirac equation as well as the Schrödinger equation [1-10]. In addition to spin, it misses the Lamb shift, the fine structure, and the hyperfine structure completely, it is not stable to radiation, and has many other problems with predictions that do not match experimentation [2-10]. It also has an infinite number of solutions, not just the ones given in textbooks as given in Margenau and Murphy [11] and Ref. [9].

Unlike physical laws such as Maxwell's equations, it is always disconcerting to those that study quantum mechanics that both must be accepted without any underlying physical basis for fundamental observables such as the stability of the hydrogen atom in the first place. In this instance, a circular argument regarding definitions for parameters in the wave equation solutions and the Rydberg series of spectral lines replaces a first-principles-based prediction of those lines [2-10].

Nevertheless, it is felt that the application of the Schrödinger equation to real problems has provided useful approximations for physicists and chemists. Schrödinger interpreted $e\Psi^*(x)\Psi(x)$ as the charge-density or the amount of charge between x and $x+dx$ (Ψ^* is the complex conjugate of Ψ). Presumably, then, he pictured the electron to be spread over large regions of space. After Schrödinger's interpretation, Max Born, who was working with scattering theory, found that this interpretation led to inconsistencies and he replaced the

Schrödinger interpretation with the probability of finding the electron between x and $x + dx$ as

$$\int \Psi(x)\Psi^*(x)dx \tag{1}$$

Born's interpretation is generally accepted. Nonetheless, interpretation of the wave function is a never-ending source of confusion and conflict. Many scientists have solved this problem by conveniently adopting the Schrödinger interpretation for some problems and the Born interpretation for others. This duality allows the electron to be everywhere at one time—yet have no volume. Alternatively, the electron can be viewed as a discrete particle that moves here and there (from $r = 0$ to $r = \infty$), and $\Psi\Psi^*$ gives the time average of this motion.

Despite its successes, quantum mechanics (QM) has remained mysterious to all who have encountered it. Starting with Bohr and progressing into the present, the departure from intuitive, physical reality has widened. The connection between quantum mechanics and reality is more than just a "philosophical" issue. It reveals that quantum mechanics is not a correct or complete theory of the physical world and that inescapable internal inconsistencies and incongruities arise when attempts are made to treat it as a physical as opposed to a purely mathematical "tool". Some of these issues are discussed in a review by Laloë [1].

But, QM has severe limitations even as a tool. Beyond one-electron atoms, multielectron-atom-quantum-mechanical equations can not be solved except by approximation methods [12] involving adjustable-parameter theories (perturbation theory, variational methods, self-consistent field method, multi-configuration Hartree Fock method, multi-configuration parametric potential method, $1/Z$ expansion method, multi-configuration Dirac-Fock method, electron correlation terms, QED terms, etc.)—all of which contain assumptions that can not be physically tested and are not consistent with physical laws. And, calling the substitutes

approximations is misleading. They are not approximations since they involve new physics or constructs or are simply curve fitting algorithms as discussed previously [6]. With adjustable parameter methods, it is necessary to repeat trial-and-error experimentation to find which method of calculation gives the right answer. It is common practice to present only the successful procedure as if it followed from first principles; and do not mention the actual method by which it was found. In many cases, the success of quantum mechanics can be attributed to the use of arbitrary variational parameters in all-space probability wave functions and arbitrary renormalization of intrinsic infinities in the corresponding energies. Furthermore, the distinction between series expansion or variation of a physical parameter of an equation based on a physical action versus the fabrication of actions based on untestable constructs corresponding to a series with variational (adjustable) parameters is discussed in Sec. II.

Also, after decades of futility, QM and the intrinsic Heisenberg Uncertainty Principle have not yielded a unified theory, are still purely mathematical, and have yet to be shown to be based in reality [2, 7, 9]. Both are based on circular arguments that the electron is a point with no volume with a vague probability wave requiring that the electron have infinite numbers of positions and energies including negative and infinite energies simultaneously. It may be time to revisit the 75 year old notion that fundamental particles such as the electron are one or zero dimensional and obey different physical laws than objects comprised of fundamental particles and the even more disturbing view that fundamental particles don't obey physical laws—rather they obey mathematics devoid of physical laws. Perhaps mathematics does not determine physics. It only models physics.

The Schrödinger equation was originally postulated in 1926 as having a solution of the one electron atom. It gives the principal energy levels of the hydrogen atom as eigenvalues of

eigenfunction solutions of the Laguerre differential equation. But, as the principal quantum number n>>1, the eigenfunctions become nonsensical since they are sinusoidal over all space; thus, they are nonintegrable, can not be normalized, and are infinite [13]. Despite its wide acceptance, on deeper inspection, the Schrödinger equation solution is plagued with many failings as well as difficulties in terms of a physical interpretation that have caused it to remain controversial since its inception. Only the one electron atom may be solved without approximations, the results are very poor, and it fails to predict electron spin and leads to models with nonsensical consequences such as negative energy states of the vacuum, infinities, and negative kinetic energy. In addition to many predictions, which simply do not agree with observations, the Schrödinger equation and succeeding extensions predict noncausality, nonlocality, spooky actions at a distance or quantum telepathy, perpetual motion, and many internal inconsistencies where contradicting statements have to be taken true simultaneously [2, 7, 9].

It was reported previously [9] that the behavior of free electrons in superfluid helium has again forced the issue of the meaning of the wavefunction. Electrons form bubbles in superfluid helium which reveal that the electron is real and that a physical interpretation of the wavefunction is necessary. Furthermore, when irradiated with light of energy of about a 0.5 to several electron volts [9, 14], the electrons carry current at different rates as if they exist with different sizes. The nature of the wavefunction needs to be addressed. It is time for the physical rather than the mathematical nature of the wavefunction to be determined. A classical derivation based on an extended electron was shown previously to be in complete agreement with observations; whereas, quantum mechanics has no utility [7, 9].

From the time of its inception, quantum mechanics (QM) has been controversial because

its foundations are in conflict with physical laws and are internally inconsistent. Interpretations of quantum mechanics such as hidden variables, multiple worlds, consistency rules, and spontaneous collapse have been put forward in an attempt to base the theory in reality. Unfortunately many theoreticians ignore the requirement that the wave function must be real and physical in order for it to be considered a valid description of reality. For example, regarding this issue Fuchs and Peres believe [15] "Contrary to those desires, quantum theory does *not* describe physical reality. What it does is provide an algorithm for computing *probabilities* for macroscopic events ("detector ticks") that are the consequences of our experimental interventions. This strict definition of the scope of quantum theory is the only interpretation ever needed, whether by experimenters or theorists".

With Penning traps, it is possible to measure transitions including those with hyperfine levels of electrons of single ions. This case can be experimentally distinguished from statistics over equivalent transitions in many ions. Whether many or one, the transition energies are always identical within the resonant line width. So, *probabilities* have no place in describing atomic energy levels. Moreover, quantum theory is incompatible with probability theory since it is based on underlying unknown, but determined outcomes as discussed previously [9].

Wavefunction solutions of the Schrödinger equation are interpreted as probability-density functions. Quantum theory confuses the concepts of a wave and a probability-density function that are based on totally different mathematical and physical principles. The use of "probability" in this instance does not conform to the mathematical rules and principles of probability theory. Statistical theory is based on an existing deterministic reality with incomplete information; whereas, quantum measurement acts on a "probability-density function" to determine a reality that did not exist before the measurement. Additionally, it is nonsensical to treat a single particle

such as an electron as if it was a population of electrons and to assign the single electron to a statistical distribution over many states. The electron has conjugate degrees of freedom such as position, momentum, and energy that obey conservation laws in an inverse-r Coulomb field. A single electron cannot have multiple positions and momenta or energies simultaneously.

The Copenhagen interpretation provides another meaning of quantum mechanics. It asserts that what we observe is all we can know; any speculation about what an electron, photon, atom, or other atomic-sized entity is really or what it is doing when we are not looking is just that—speculation. The postulate of quantum measurement asserts that the process of measuring an observable forces it into a state of reality. In other words, reality is irrelevant until a measurement is made. In the case of electrons in superfluid helium, the fallacy with this position is that the "ticks" (migration times of electron bubbles) reveal that the electron is real before a measurement is made. Furthermore, experiments on transitions on single ions such as Ba^+ in a Penning trap under continuous observation demonstrate that the postulate of quantum measurement of quantum mechanics is experimentally disproved as discussed previously [9, 16]. These issues and other such flawed philosophies and interpretations of experiments that arise from quantum mechanics were discussed previously [1-10].

QM gives correlations with experimental data. It does not explain the mechanism for the observed data. But, it should not be surprising that it may give good correlations given that the constraints of internal consistency and conformance to physical laws are removed for a wave equation with an infinite number of solutions wherein the solutions may be formulated as an infinite series of eigenfunctions with variable parameters. There are no physical constraints on the parameters. They may even correspond to unobservables such as virtual particles, hyperdimensions, effective nuclear charge, polarization of the vacuum, worm holes, spooky

action at a distance, infinities, parallel universes, faster than light travel, etc. If you invoke the constraints of internal consistency and conformance to physical laws, quantum mechanics has never successfully solved a physical problem as discussed previously [6].

Reanalysis of old experiments and many new experiments including electrons in superfluid helium challenge the Schrödinger equation predictions. Many noted physicists rejected quantum mechanics. Feynman also attempted to use first principles including Maxwell's equations to discover new physics to replace quantum mechanics [17]. Other great physicists of the 20th century searched. "Einstein [...] insisted [...] that a more detailed, wholly deterministic theory must underlie the vagaries of quantum mechanics" [18]. He felt that scientists were misinterpreting the data. These issues and the results of many experiments such as the wave-particle duality, the Lamb shift, anomalous magnetic moment of the electron, transition and decay lifetimes, experiments invoking interpretations of spooky action at a distance such as the Aspect experiment, entanglement, and double-slit-type experiments are shown to be absolutely predictable and physical in the context of a theory of classical quantum mechanics (CQM) derived from first principles [2-10].

II. Quantum Electrodynamics (QED)

Quantum mechanics failed to predict the results of the Stern-Gerlach experiment which indicated the need for an additional quantum number. In quantum mechanics, the spin angular momentum of the electron is called the "intrinsic angular momentum" since no physical interpretation exists. (Currents corresponding to the observed magnetic field of the electron can not exist in one dimension of four dimensional spacetime where Ampere's law and the intrinsic special relativity determine the corresponding unique current.) The Schrödinger equation is not

Lorentzian invariant in violation of special relativity. The Schrödinger equation also misses the Lamb shift, the fine structure, and the hyperfine structure completely, and it is not stable to radiation. Quantum electrodynamics was proposed by Dirac in 1926 to provide a generalization of quantum mechanics for high energies in conformity with the theory of special relativity and to provide a consistent treatment of the interaction of matter with radiation. But, it does not bridge the gap between quantum mechanics and special relativity. From Weisskopf [19], "Dirac's quantum electrodynamics gave a more consistent derivation of the results of the correspondence principle, but it also brought about a number of new and serious difficulties." Quantum electrodynamics: (1) does not explain nonradiation of bound electrons; (2) contains an internal inconsistency with special relativity regarding the classical electron radius—the electron mass corresponding to its electric energy is infinite; (3) admits solutions of negative rest mass and negative kinetic energy; (4) leads to infinite kinetic energy and infinite electron mass for the interaction of the electron with the predicted zero-point field fluctuations (5) still yielded infinities when Dirac used the unacceptable states of negative mass for the description of the vacuum. Dirac's postulated relativistic wave equation gives the inescapable result of a cosmological constant that is at least 120 orders of magnitude larger than the best observational limit due to the unacceptable states of negative mass for the description of the vacuum as discussed previously [2-7, 9-10][1]. The negative mass states further create an absolute "ether"-

[1] The Rutherford experiment demonstrated that even atoms are comprised of essentially empty space [20]. Zero-point field fluctuations, virtual particles, and states of negative energy and mass invoked to describe the vacuum are nonsensical and have no basis in reality since they have never been observed experimentally and would correspond to an essentially infinite cosmological constant throughout the entire universe including regions of no mass. As given by Waldrop [21], "What makes this problem into something more than metaphysics is that the cosmological constant is observationally zero to a very high degree of accuracy. And yet, ordinary quantum field theory predicts that it ought to be enormous, about 120 orders of magnitude larger than the best observational limit. Moreover, this prediction is almost inescapable because it is a

like frame in violation of special relativity which was disproved by the Michelson-Morley experiment.

In retrospect, Dirac's equation which was postulated to explain spin relies on the unfounded notions of negative energy states of the vacuum, virtual particles, and gamma factors; thus, it can not be the correct description of a bound electron even though it gives an addition quantum number interpreted as corresponding to the phenomenon of electron spin. Ironically, it is not even internally consistent with respect to its intent of being in accord with special relativity. The Dirac equation violates Maxwell's equations with respect to stability to radiation, contains an internal inconsistency with special relativity regarding the classical electron radius and states of negative rest mass and negative kinetic energy as given by Weisskopf [19], and further violates Einstein causality and locality in addition to conservation of energy as shown by the Klein Paradox discussed previously [2, 4, 7][2]. Furthermore, everyday observation demonstrates that causality and locality always hold. Einstein also argued that a probabilistic versus deterministic nature of atomic particles leads to disagreement with special relativity. In

---

straightforward application of the uncertainty principle, which in this case states that every quantum field contains a certain, irreducible amount of energy even in empty space. Electrons, photons, quarks—the quantum field of every particle contributes. And that energy is exactly equivalent to the kind of pressure described by the cosmological constant. The cosmological constant has accordingly been an embarrassment and a frustration to every physicist who has ever grappled with it."

[2] Oskar Klein pointed out a glaring paradox implied by the Dirac equation which was never resolved [23]. "Electrons may penetrate an electrostatic barrier even when their kinetic energy, $E - mc^2$ is lower than the barrier. Since in Klein's example the barrier was infinitely broad this could not be associated with wave mechanical tunnel effect. It is truly a paradox: Electrons too slow to surpass the potential, may still only be partially reflected. ...Even for an infinitely high barrier, i.e. $r_2 = 1$ and energies $\approx 1\,MeV$, (the reflection coefficient) R is less than 75%! From (2) and (3) it appears that as soon as the barrier is sufficiently high: $V > 2mc^2$, electrons may transgress the repulsive wall—seemingly defying conservation of energy. ...Nor is it possible by way of the positive energy spectrum of the free electron to achieve complete Einstein causality."

fact, the nonlocality result of the Copenhagen interpretation violates causality as shown by Einstein, Podolsky, and Rosen (EPR) in a classic paper [22] that presented a paradox involving instantaneous (faster-than-light) communication between particles called "spooky action at a distance" which led them to conclude that quantum mechanics is not a complete or correct theory. The implications of the EPR paper and the exact Maxwellian predictions of "spooky action" and "entanglement" experiments, incorrectly interpreted in the context of quantum mechanic, are given in Chp. 37 of Ref. [7].

In 1947, contrary to Dirac's predictions, Lamb discovered a 1000 *MHz* shift between the $^2S_{1/2}$ state and the $^2P_{1/2}$ state of the hydrogen atom [24]. This so called Lamb Shift marked the beginning of modern quantum electrodynamics. In the words of Dirac [25], "No progress was made for 20 years. Then a development came initiated by Lamb's discovery and explanation of the Lamb Shift, which fundamentally changed the character of theoretical physics. It involved setting up rules for discarding ...infinities..." Renormalization is presently believed to be required of any fundamental theory of physics [26]. However, dissatisfaction with renormalization has been expressed at various times by many physicists including Dirac [27] who felt that, "This is just not sensible mathematics. Sensible mathematics involves neglecting a quantity when it turns out to be small—not neglecting it just because it is infinitely great and you do not want it!"

Albeit, the Dirac equation did not predict the Lamb shift or the electron g factor [24, 28-29], its feature of negative-mass states of the vacuum gave rise to the postulates of QED that has become a center piece of quantum mechanics to explain these and other similar observations. One of QED's seminal aspects of renormalization which was subsequently grafted into atomic theory was a turning point in physics similar to the decision to treat the electron as a point-

particle-probability wave, a point with no volume with a vague probability wave requiring that the electron have an infinite number of positions and energies including negative and infinite energies simultaneously. The adoption of the probabilistic versus deterministic nature of atomic particles violates all physical laws including special relativity with violation of causality as pointed out by Einstein [22] and de Broglie [30]. Consequently, it was rejected even by Schrödinger [31].

Pure mathematics took the place of physics when calculating subtle shifts of the hydrogen atomic energy levels. Moreover, in QED, the pure mathematics approach has been confused with physics to the point that virtual particles are really considered as causing the observable. The justification for the linkage is often incorrectly associated with the usage of series expansion and variational methods to solve problems based on physical laws. But, series expansion of an equation based on a physical action or variation of a physical parameter of the equation versus the fabrication of an action based on fantastical untestable constructs that are represented by a series are clearly different. For example, the motion of a pendulum can be solved exactly in terms of an elliptic integral using Newtonian mechanics. Expansion of the elliptic integral in a power series and ignoring negligible terms in the series versus setting up of arbitrary rules for *discarding infinities* are clearly not the same. Furthermore, inventing virtual particles that have an action on space, and subsequently on an electron, versus expanding terms in the energy equation due to a gravitating body causing a gravitational field and thus an action on the pendulum are very different. In QED, virtual particles are not merely a sustitutional or expansion variable. They are really considered as causing the observable.

In a further exercise of poor science, virtual-particle-based calculations are even included in the determination of the fundamental constants which are circularly used to calculate the

parameter ascribed to the virtual particles. For example, using the electron magnetic moment anomaly in the selection of the best value of the fine structure constant, the CODATA publication [32] reports the use of virtual particles:

> "The term A1 is mass independent and the other terms are functions of the indicated mass ratios. For these terms the lepton in the numerator of the mass ratio is the particle under consideration, while the lepton in the denominator of the ratio is the virtual particle that is the source of vacuum polarization that gives rise to the term."

There is no direct evidence that virtual particles exist or that they polarize the vacuum. Even their postulation is an oxymoron.

Throughout the history of quantum theory, wherever there was an advance to a new application, it was necessary to repeat a trial-and -error experimentation to find which method of calculation gave the right answers. Often the textbooks present only the successful procedure as if it followed from first principles and do not mention the actual method by which it was found. In electromagnetic theory based on Maxwell's equations, one deduces the computational algorithm from the general principles. In quantum theory, the logic is just the opposite. One chooses the principle (e.g. phenomenological Hamiltonians) to fit the empirically successful algorithm. For example, we know that it required a great deal of art and tact over decades of effort to get correct predictions out of QED. The QED method of the determination of $(g-2)/2$ from the *postulated* Dirac equation is based on a *postulated* power series of α/π where each *postulated* virtual particle is a source of *postulated* vacuum polarization that gives rise to a *postulated* term which is processed over decades using ad hoc rules to remove infinities from each term that arises from *postulated* scores of *postulated* Feynman diagrams. The solution so obtained using the perturbation series further requires a *postulated* truncation since the series *diverges*. Mohr and Taylor reference some of the Herculean efforts to arrive at g using QED

[32]:

"the sixth-order coefficient $A_1^{(6)}$ arises from 72 diagrams and is also known analytically after nearly 30 years of effort by many researchers [see Roskies, Remiddi, and Levine (1990) for a review of the early work]. It was not until 1996 that the last remaining distinct diagrams were calculated analytically, thereby completing the theoretical expression for $A_1^{(6)}$".

For the right experimental numbers to emerge, one must do the calculation (i.e. subtract off the infinities) in one particular way and not in some other way that appears in principle equally valid. For example, Milonni [33] presents a QED derivation of the magnetic moment of the electron which gives a result of the wrong sign and requires the introduction of an

"upper limit K in the integration over $k = \omega / c$ in order to avoid a divergence."

A differential mass is arbitrarily added, then

"the choice $K = 0.42mc/\hbar$ yields $(g-2)/2 = \alpha/2\pi$ which is the relativistic QED result to first order in α. [...] However, the reader is warned not to take these calculations too seriously, for the result $(g-2)/2 = \alpha/2\pi$ could be obtained by retaining only the first (radiation reaction) term in (3.112) and choosing $K = 3mc/8\hbar$. It should also be noted that the solution $K \cong 0.42mc/\hbar$ of (3.112) with $(g-2)/2 = \alpha/2\pi$ is not unique."

Such an ad hoc nonphysical approach makes incredulous:

" the cliché that QED is the best theory we have!" [34]

or the statement that:

"The history of quantum electrodynamics (QED) has been one of unblemished triumph" [35].

There is a corollary, noted by Kallen: from an inconsistent theory, any result may be derived.

In an attempt to provide some physical insight into atomic problems and starting with the same essential physics as Bohr of e^- moving in the Coulombic field of the proton and the wave equation as modified after Schrödinger, a classical approach was explored which yields a model

which is remarkably accurate and provides insight into physics on the atomic level [2-7]. Physical laws and intuition are restored when dealing with the wave equation and quantum mechanical problems. Specifically, a theory of classical quantum mechanics (CQM) was derived from first principles that successfully applies physical laws on all scales. Rather than use the postulated Schrödinger boundary condition: "$\Psi \to 0$ as $r \to \infty$", which leads to a purely mathematical model of the electron, the constraint is based on experimental observation. Using Maxwell's equations, *the classical wave equation is solved with the constraint that the bound* $n = 1$*-state electron cannot radiate energy*. The electron must be extended rather than a point. On this basis with the assumption that physical laws including Maxwell's equation apply to bound electrons, the hydrogen atom was solved exactly from first principles. The remarkable agreement across the spectrum of experimental results indicates that this is the correct model of the hydrogen atom.

It was shown previously that quantum mechanics does not explain the stability of the atom to radiation [2]; whereas, the Maxwellian approach gives a natural relationship between Maxwell's equations, special relativity, and general relativity. CQM holds over a scale of spacetime of 85 orders of magnitude—it correctly predicts the nature of the universe from the scale of the quarks to that of the cosmos [3]. A review is given by Landvogt [36]. In a third paper, the atomic physical approach was applied to multielectron atoms that were solved exactly disproving the deep-seated view that such exact solutions can not exist according to quantum mechanics. The general solutions for one through twenty-electron atoms are given in Ref [4]. The predictions are in remarkable agreement with the experimental values known for 400 atoms and ions. A fourth paper presents a solution based on physical laws and fully compliant with Maxwell's equations that solves the 26 parameters of molecular ions and molecules of hydrogen

isotopes in closed-form equations with fundamental constants only that match the experimental values [5]. In a fifth paper, the nature of atomic physics being correctly represented by quantum mechanics versus classical quantum mechanics is subjected to a test of internal consistency for the ability to calculate the conjugate observables using the same solution for each of the separate experimental measurements [6]. It is confirmed that the CQM solution is the accurate model of the helium atom by the agreement of predicted and observed conjugate parameters of the free electron, ionization energy of helium and all two electron atoms, ionization energies of multielectron atoms, electron scattering of helium for all angles, and all He I excited states using the same unique physical model in all cases. Over five hundred conjugate parameters are calculated using a unique solution of the two-electron atom without any adjustable parameters. In the closed-form equations, overall agreement is achieved to the level obtainable considering the error in the measurements and in the fundamental constants.

In contrast, the quantum fails utterly. Ad hoc computer algorithms are used to generate meaningless numbers with internally inconsistent and nonphysical models that have no relationship to physics. Attempts are often made to numerically reproduce prior theoretical numbers using adjustable parameters including arbitrary wave functions in computer programs with precision that is often much greater (e.g. 8 significant figures greater) than possible based on the propagation of errors in the measured fundamental constants implicit in the physical problem.

In this sixth paper of a series, rather than invoking renormalization, untestable virtual particles, and polarization of the vacuum by the virtual particles, the results of QED such as the anomalous magnetic moment of the electron, the Lamb Shift, the fine structure and hyperfine structure of the hydrogen atom, and the hyperfine structure intervals of positronium and

muonium (thought to be only solvable using QED) are solved exactly from Maxwell's equations to the limit possible based on experimental measurements.

III. Classical Quantum Theory of the Atom Based on Maxwell's Equations

In this paper, the old view that the electron is a zero or one-dimensional point in an all-space probability wave function $\Psi(x)$ is not taken for granted. The theory of classical quantum mechanics (CQM), derived from first principles, must successfully and consistently apply physical laws on all scales [2-10]. Stability to radiation was ignored by all past atomic models. Historically, the point at which QM broke with classical laws can be traced to the issue of nonradiation of the one electron atom. Bohr just postulated orbits stable to radiation with the further postulate that the bound electron of the hydrogen atom does not obey Maxwell's equations—rather it obeys different physics [2, 7]. Later physics was replaced by "pure mathematics" based on the notion of the inexplicable wave-particle duality nature of electrons which lead to the Schrödinger equation wherein the consequences of radiation predicted by Maxwell's equations were ignored. Ironically, Bohr, Schrödinger, and Dirac used the Coulomb potential, and Dirac used the vector potential of Maxwell's equations. But, all ignored electrodynamics and the corresponding radiative consequences. Dirac originally attempted to solve the bound electron physically with stability with respect to radiation according to Maxwell's equations with the further constraints that it was relativistically invariant and gave rise to electron spin [37]. He and many founders of QM such as Sommerfeld, Bohm, and Weinstein wrongly pursued a planetary model, were unsuccessful, and resorted to the current mathematical-probability-wave model that has many problems [1-10, 19, 22-23, 37]. Consequently, Feynman for example, attempted to use first principles including Maxwell's

equations to discover new physics to replace quantum mechanics [38].

Physical laws may indeed be the root of the observations thought to be "purely quantum mechanical", and it may have been a mistake to make the assumption that Maxwell's electrodynamic equations must be rejected at the atomic level. Thus, in the present approach, the classical wave equation is solved with the constraint that a bound $n = 1$-state electron cannot radiate energy.

Herein, derivations consider the electrodynamic effects of moving charges as well as the Coulomb potential, and the search is for a solution representative of the electron wherein there is acceleration of charge motion without radiation. The mathematical formulation for zero radiation based on Maxwell's equations follows from a derivation by Haus [39]. The function that describes the motion of the electron must not possess spacetime Fourier components that are synchronous with waves traveling at the speed of light. Similarly, nonradiation is demonstrated based on the electron's electromagnetic fields and the Poynting power vector.

It was shown previously [3-8] that CQM gives closed form solutions for the atom including the stability of the $n = 1$ state and the instability of the excited states, the equation of the photon and electron in excited states, the equation of the free electron, and photon which predict the wave particle duality behavior of particles and light. The current and charge density functions of the electron may be directly physically interpreted. For example, spin angular momentum results from the motion of negatively charged mass moving systematically, and the equation for angular momentum, $\mathbf{r} \times \mathbf{p}$, can be applied directly to the wave function (a current density function) that describes the electron. The magnetic moment of a Bohr magneton, Stern Gerlach experiment, g factor, Lamb shift, resonant line width and shape, selection rules, correspondence principle, wave particle duality, excited states, reduced mass, rotational energies,

and momenta, orbital and spin splitting, spin-orbital coupling, Knight shift, and spin-nuclear coupling, and elastic electron scattering from helium atoms, are derived in closed form equations based on Maxwell's equations. The calculations agree with experimental observations.

In contrast to the failure of the Bohr theory and the nonphysical, adjustable-parameter approach of quantum mechanics, multielectron atoms [4, 7] and the nature of the chemical bond [5, 7] are given by exact closed-form solutions containing fundamental constants only. Using the nonradiative wave equation solutions that describe each bound electron having conserved momentum and energy, the radii are determined from the force balance of the electric, magnetic, and centrifugal forces that correspond to the minimum of energy of the atomic or ionic system. The ionization energies are then given by the electric and magnetic energies at these radii. The spreadsheets to calculate the energies from exact solutions of one through twenty-electron atoms are available from the internet [40]. For 400 atoms and ions the agreement between the predicted and experimental results are remarkable.

A. One-Electron Atoms

One-electron atoms include the hydrogen atom, He^{+}, Li^{2+}, Be^{3+}, and so on. The mass-energy and angular momentum of the electron are constant; this requires that the equation of motion of the electron be temporally and spatially harmonic. Thus, the classical wave equation applies and

$$\left[\nabla^2 - \frac{1}{v^2}\frac{\partial^2}{\partial t^2}\right]\rho(r,\theta,\phi,t) = 0 \qquad (2)$$

where $\rho(r,\theta,\phi,t)$ is the time dependent charge density function of the electron in time and space. In general, the wave equation has an infinite number of solutions. To arrive at the

solution which represents the electron, a suitable boundary condition must be imposed. It is well known from experiments that each single atomic electron of a given isotope radiates to the same stable state. Thus, the physical boundary condition of nonradiation of the bound electron was imposed on the solution of the wave equation for the time dependent charge density function of the electron [2-8]. The condition for radiation by a moving point charge given by Haus [39] is that its spacetime Fourier transform does possess components that are synchronous with waves traveling at the speed of light. Conversely, it is proposed that the condition for nonradiation by an ensemble of moving point charges that comprises a current density function is

For non-radiative states, the current-density function must NOT possess spacetime Fourier components that are synchronous with waves traveling at the speed of light.

The time, radial, and angular solutions of the wave equation are separable. The motion is time harmonic with frequency ω_n. A constant angular function is a solution to the wave equation. Solutions of the Schrödinger wave equation comprising a radial function radiate according to Maxwell's equation as shown previously by application of Haus' condition [39]. In fact, it was found that any function which permitted radial motion gave rise to radiation. A radial function which does satisfy the boundary condition is a radial delta function

$$f(r) = \frac{1}{r^2}\delta(r - r_n) \tag{3}$$

This function defines a constant charge density on a spherical shell where $r_n = nr_1$ wherein n is an integer in an excited state, and Eq. (2) becomes the two-dimensional wave equation plus time with separable time and angular functions. Given time harmonic motion and a radial delta function, the relationship between an allowed radius and the electron wavelength is given by

$$2\pi r_n = \lambda_n \tag{4}$$

where the integer subscript n here and in Eq. (3) is determined during photon absorption as given in the Excited States of the One-Electron Atom (Quantization) section of Ref. [7]. Using the observed de Broglie relationship for the electron mass where the coordinates are spherical,

$$\lambda_n = \frac{h}{p_n} = \frac{h}{m_e v_n} \tag{5}$$

and the magnitude of the velocity for *every* point on the orbitsphere is

$$v_n = \frac{\hbar}{m_e r_n} \tag{6}$$

The sum of the $|\mathbf{L}_i|$, the magnitude of the angular momentum of each infinitesimal point of the orbitsphere of mass m_i, must be constant. The constant is $\hbar$.

$$\sum |\mathbf{L}_i| = \sum |\mathbf{r} \times m_i \mathbf{v}| = m_e r_n \frac{\hbar}{m_e r_n} = \hbar \tag{7}$$

Thus, an electron is a spinning, two-dimensional spherical surface (zero thickness), called an *electron orbitsphere* shown in Figure 1, that can exist in a bound state at only specified distances from the nucleus determined by an energy minimum. The corresponding current function shown in Figure 2 which gives rise to the phenomenon of *spin* is derived in the Spin Function section. (See the Orbitsphere Equation of Motion for $\ell = 0$ of Ref. [7] at Chp. 1.)

Nonconstant functions are also solutions for the angular functions. To be a harmonic solution of the wave equation in spherical coordinates, these angular functions must be spherical harmonic functions [41]. A zero of the spacetime Fourier transform of the product function of two spherical harmonic angular functions, a time harmonic function, and an unknown radial function is sought. The solution for the radial function which satisfies the boundary condition is also a delta function given by Eq. (3). Thus, bound electrons are described by a charge-density

(mass-density) function which is the product of a radial delta function, two angular functions (spherical harmonic functions), and a time harmonic function.

$$\rho(r,\theta,\phi,t) = f(r)A(\theta,\phi,t) = \frac{1}{r^2}\delta(r-r_n)A(\theta,\phi,t); \qquad A(\theta,\phi,t) = Y(\theta,\phi)k(t) \tag{8}$$

In these cases, the spherical harmonic functions correspond to a traveling charge density wave confined to the spherical shell which gives rise to the phenomenon of orbital angular momentum. The orbital functions which modulate the constant "spin" function shown graphically in Figure 3 are given in the Sec. IIIC.

B. Spin Function

The orbitsphere spin function comprises a constant charge (current) density function with moving charge confined to a two-dimensional spherical shell. The magnetostatic current pattern of the orbitsphere spin function comprises an infinite series of correlated orthogonal great circle current loops wherein each point charge (current) density element moves time harmonically with constant angular velocity

$$\omega_n = \frac{\hbar}{m_e r_n^2} \tag{9}$$

The uniform current density function $Y_0^0(\theta,\phi)$ that gives rise to the spin of the electron is generated from a basis set current-vector field defined as the orbitsphere current-vector field ("orbitsphere-cvf"). The orbitsphere-cvf comprises a continuum of correlated orthogonal great circle current loops. The current pattern comprising two components is generated over the surface by two sets (*Steps One and Two*) of rotations of two orthogonal great circle current loops that serve as basis elements about each of the $(\mathbf{i}_x, \mathbf{i}_y, 0\mathbf{i}_z)$ and $\left(-\frac{1}{\sqrt{2}}\mathbf{i}_x, \frac{1}{\sqrt{2}}\mathbf{i}_y, \mathbf{i}_z\right)$-axes,

respectively, by π radians. In Appendix III of Ref. [7], the *continuous* uniform electron current density function $Y_0^0(\theta,\phi)$ having the same angular momentum components as that of the orbitsphere-cvf is then exactly generated from this orbitsphere-cvf as a basis element by a convolution operator comprising an autocorrelation-type function.

The orthogonal great circle basis set for Step One is shown in Figure 4. One half of the orbitsphere-cvf, the orbitsphere-cvf component of STEP ONE, is generated by the rotation of two orthogonal great circles about the $(\mathbf{i}_x,\mathbf{i}_y,0\mathbf{i}_z)$-axis by π wherein one basis-element great circle initially is initially in the yz-plane and the other is in the xz-plane:

Step One

$$\begin{bmatrix} x' \\ y' \\ z' \end{bmatrix} = \begin{bmatrix} \frac{1}{2}+\frac{\cos\theta}{2} & \frac{1}{2}-\frac{\cos\theta}{2} & -\frac{\sin\theta}{\sqrt{2}} \\ \frac{1}{2}-\frac{\cos\theta}{2} & \frac{1}{2}+\frac{\cos\theta}{2} & \frac{\sin\theta}{\sqrt{2}} \\ \frac{\sin\theta}{\sqrt{2}} & -\frac{\sin\theta}{\sqrt{2}} & \cos\theta \end{bmatrix} \bullet \left(\begin{bmatrix} 0 \\ r_n\cos\phi \\ r_n\sin\phi \end{bmatrix} + \begin{bmatrix} r_n\cos\phi \\ 0 \\ r_n\sin\phi \end{bmatrix} \right) \tag{10}$$

The first component of the orbitsphere-cvf given by Eq. (10) can also be generated by each of rotating a great circle basis element initially in the yz or the xz-planes about the $(\mathbf{i}_x,\mathbf{i}_y,0\mathbf{i}_z)$-axis by 2π radians as shown in Figures 5 and 6, respectively.

The orthogonal great circle basis set for Step Two is shown in Figure 7. The second half of the orbitsphere-cvf, the orbitsphere-cvf component of STEP TWO, is generated by the rotation of two orthogonal great circles about the $\left(-\frac{1}{\sqrt{2}}\mathbf{i}_x,\frac{1}{\sqrt{2}}\mathbf{i}_y,\mathbf{i}_z\right)$-axis by π wherein one basis-element great circle is initially in the plane that bisects the xy-quadrant and is parallel to

the z-axis and the other is in the xy-plane:

Step Two

$$\begin{bmatrix} x' \\ y' \\ z' \end{bmatrix} = \begin{bmatrix} \frac{1}{4}(1+3\cos\theta) & \frac{1}{4}\left(-1+\cos\theta+2\sqrt{2}\sin\theta\right) & \frac{1}{4}\left(-\sqrt{2}+\sqrt{2}\cos\theta-2\sin\theta\right) \\ \frac{1}{4}\left(-1+\cos\theta-2\sqrt{2}\sin\theta\right) & \frac{1}{4}(1+3\cos\theta) & \frac{1}{4}\left(\sqrt{2}-\sqrt{2}\cos\theta-2\sin\theta\right) \\ \frac{1}{2}\left(\frac{-1+\cos\theta}{\sqrt{2}}+\sin\theta\right) & \frac{1}{4}\left(\sqrt{2}-\sqrt{2}\cos\theta+2\sin\theta\right) & \cos^2\frac{\theta}{2} \end{bmatrix} \bullet \left(\begin{bmatrix} \frac{r_n\cos\phi}{\sqrt{2}} \\ \frac{r_n\cos\phi}{\sqrt{2}} \\ r_n\sin\phi \end{bmatrix} + \begin{bmatrix} r_n\cos\phi \\ r_n\sin\phi \\ 0 \end{bmatrix} \right) \tag{11}$$

The second component of the orbitsphere-cvf given by Eq. (11) can also be generated by each of rotating a great circle basis element that is initially in the plane that bisects the xy-quadrant and is parallel to the z-axis or is in the xy-plane about the $\left(-\frac{1}{\sqrt{2}}\mathbf{i}_x, \frac{1}{\sqrt{2}}\mathbf{i}_y, \mathbf{i}_z\right)$-axis by 2π radians as shown in Figures 8 and 9, respectively.

The orbitsphere-cvf is given by the superposition of the components from Step One and from Step Two. The current pattern of the orbitsphere-cvf generated by the rotations of the orthogonal great circle current loops is a continuous and total coverage of the spherical surface, but it is shown as visual representations using 6 degree increments θ in Figures 2A-C.

The resultant angular momentum projections of $\mathbf{L}_{xy} = \frac{\hbar}{4}$ and $\mathbf{L}_z = \frac{\hbar}{2}$ meet the boundary condition for the unique current having an angular velocity magnitude at each point on the

surface given by Eq. (6) and give rise to the Stern Gerlach experiment as shown in Ref. [7]. The further constraint that the current density is uniform such that the charge density is uniform, corresponding to an equipotential, minimum energy surface is satisfied by using the orbitsphere-cvf as a basis element to generate $Y_0^0(\phi,\theta)$ using a convolution operator comprising an autocorrelation-type function as given in Appendix III of Ref. [7]. The operator comprises the convolution of each great circle current loop of the orbitsphere-cvf designated as the primary orbitsphere-cvf with a second orbitsphere-cvf designated as the secondary orbitsphere-cvf wherein the convolved secondary elements are matched for orientation, angular momentum, and phase to those of the primary. The resulting exact uniform current distribution obtained from the convolution has the same angular momentum distribution, resultant, $\mathbf{L_R}$, and components of $\mathbf{L}_{xy} = \frac{\hbar}{4}$ and $\mathbf{L}_z = \frac{\hbar}{2}$ as those of the orbitsphere-cvf used as a primary basis element.

C. Angular Functions

The time, radial, and angular solutions of the wave equation are separable. Also based on the radial solution, the angular charge and current-density functions of the electron, $A(\theta,\phi,t)$, must be a solution of the wave equation in two dimensions (plus time),

$$\left[\nabla^2 - \frac{1}{v^2}\frac{\partial^2}{\partial t^2}\right] A(\theta,\phi,t) = 0 \tag{12}$$

where $\rho(r,\theta,\phi,t) = f(r)A(\theta,\phi,t) = \frac{1}{r^2}\delta(r-r_n)A(\theta,\phi,t)$ and $A(\theta,\phi,t) = Y(\theta,\phi)k(t)$

$$\left[\frac{1}{r^2\sin\theta}\frac{\partial}{\partial\theta}\left(\sin\theta\frac{\partial}{\partial\theta}\right)_{r,\phi} + \frac{1}{r^2\sin^2\theta}\left(\frac{\partial^2}{\partial\phi^2}\right)_{r,\theta} - \frac{1}{v^2}\frac{\partial^2}{\partial t^2}\right] A(\theta,\phi,t) = 0 \tag{13}$$

where v is the linear velocity of the electron. The charge-density functions including the time-

function factor are

$\ell = 0$

$$\rho(r,\theta,\phi,t) = \frac{e}{8\pi r^2}[\delta(r - r_n)]\left[Y_0^0(\theta,\phi) + Y_\ell^m(\theta,\phi)\right] \tag{14}$$

$\ell \neq 0$

$$\rho(r,\theta,\phi,t) = \frac{e}{4\pi r^2}[\delta(r - r_n)]\left[Y_0^0(\theta,\phi) + \mathrm{Re}\left\{Y_\ell^m(\theta,\phi)e^{i\omega_n t}\right\}\right] \tag{15}$$

where $Y_\ell^m(\theta,\phi)$ are the spherical harmonic functions that spin about the z-axis with angular frequency ω_n with $Y_0^0(\theta,\phi)$ the constant function. $\mathrm{Re}\left\{Y_\ell^m(\theta,\phi)e^{i\omega_n t}\right\} = P_\ell^m(\cos\theta)\cos\left(m\phi + \omega_n' t\right)$ where to keep the form of the spherical harmonic as a traveling wave about the z-axis, $\omega_n' = m\omega_n$.

D. Acceleration without Radiation

a. Special Relativistic Correction to the Electron Radius

The relationship between the electron wavelength and its radius is given by Eq. (4) where λ is the de Broglie wavelength. For each current density element of the spin function, the distance along each great circle in the direction of instantaneous motion undergoes length contraction and time dilation. Using a phase matching condition, the wavelengths of the electron

and laboratory inertial frames are equated, and the corrected radius is given by

$$r_n = r_n^{'}\left[\sqrt{1-\left(\frac{v}{c}\right)^2}\,\sin\left[\frac{\pi}{2}\left(1-\left(\frac{v}{c}\right)^2\right)^{3/2}\right]+\frac{1}{2\pi}\cos\left[\frac{\pi}{2}\left(1-\left(\frac{v}{c}\right)^2\right)^{3/2}\right]\right] \tag{16}$$

where the electron velocity is given by Eq. (6). (See Ref. [7] Chp. 1, Special Relativistic Correction to the Ionization Energies section). $\frac{e}{m_e}$ of the electron, the electron angular momentum of $\hbar$, and μ_B are invariant, but the mass and charge densities increase in the laboratory frame due to the relativistically contracted electron radius. As $v \to c$, $r/r' \to \frac{1}{2\pi}$ and $r = \lambda$ as shown in Figure 10.

b. Nonradiation Based on the Spacetime Fourier Transform of the Electron Current

The Fourier transform of the electron charge density function given by Eq. (8) is a solution of the three-dimensional wave equation in frequency space ($\mathbf{k}, \omega\, space$) as given in Chp 1, Spacetime Fourier Transform of the Electron Function section of Ref. [7]. Then the corresponding Fourier transform of the current density function $K(s,\Theta,\Phi,\omega)$ is given by multiplying by the constant angular frequency.

$$\begin{aligned} K(s,\Theta,\Phi,\omega) = 4\pi\omega_n \frac{\sin(2s_n r_n)}{2s_n r_n} \otimes 2\pi\sum_{\upsilon=1}^{\infty} \frac{(-1)^{\upsilon-1}(\pi\sin\Theta)^{2(\upsilon-1)}}{(\upsilon-1)!(\upsilon-1)!}\frac{\Gamma\left(\frac{1}{2}\right)\Gamma\left(\upsilon+\frac{1}{2}\right)}{(\pi\cos\Theta)^{2\upsilon+1}2^{\upsilon+1}}\frac{2\upsilon!}{(\upsilon-1)!}s^{-2\upsilon} \\ \otimes 2\pi\sum_{\upsilon=1}^{\infty} \frac{(-1)^{\upsilon-1}(\pi\sin\Phi)^{2(\upsilon-1)}}{(\upsilon-1)!(\upsilon-1)!}\frac{\Gamma\left(\frac{1}{2}\right)\Gamma\left(\upsilon+\frac{1}{2}\right)}{(\pi\cos\Phi)^{2\upsilon+1}2^{\upsilon+1}}\frac{2\upsilon!}{(\upsilon-1)!}s^{-2\upsilon}\frac{1}{4\pi}[\delta(\omega-\omega_n)+\delta(\omega+\omega_n)] \end{aligned} \tag{17}$$

$\mathbf{s}_n \bullet \mathbf{v}_n = \mathbf{s}_n \bullet \mathbf{c} = \omega_n$ implies $r_n = \lambda_n$ which is given by Eq. (16) in the case that k is the lightlike

k^0. In this case, Eq. (17) vanishes. Consequently, spacetime harmonics of $\frac{\omega_n}{c} = k$ or $\frac{\omega_n}{c}\sqrt{\frac{\varepsilon}{\varepsilon_o}} = k$ for which the Fourier transform of the current-density function is nonzero do not exist. Radiation due to charge motion does not occur in any medium when this boundary condition is met. Nonradiation is also determined directly from the fields based on Maxwell's equations as given in Sec. IIIDc.

c. Nonradiation Based on the Electron Electromagnetic Fields and the Poynting Power Vector

A point charge undergoing periodic motion accelerates and as a consequence radiates according to the Larmor formula:

$$P = \frac{1}{4\pi\varepsilon_0}\frac{2e^2}{3c^3}a^2 \tag{18}$$

where e is the charge, a is its acceleration, ε_0 is the permittivity of free space, and c is the speed of light. Although an accelerated *point* particle radiates, an *extended distribution* modeled as a superposition of accelerating charges does not have to radiate [37, 39, 42-44]. In Ref. [3] and Appendix I, Chp. 1 of Ref. [7], the electromagnetic far field is determined from the current distribution in order to obtain the condition, if it exists, that the electron current distribution must satisfy such that the electron does not radiate. The current follows from Eqs. (14-15). The currents corresponding to Eq. (14) and first term of Eq. (15) are static. Thus, they are trivially nonradiative. The current due to the time dependent term of Eq. (15) corresponding to p, d, f, etc. orbitals is

$$\mathbf{J} = \frac{\omega_n}{2\pi}\frac{e}{4\pi r_n^2} N[\delta(r-r_n)]\,\mathrm{Re}\left\{Y_\ell^m(\theta,\phi)\right\}[\mathbf{u}(t)\times\mathbf{r}]$$
$$= \frac{\omega_n}{2\pi}\frac{e}{4\pi r_n^2} N'[\delta(r-r_n)]\left(P_\ell^m(\cos\theta)\cos\left(m\phi+\omega_n' t\right)\right)[\mathbf{u}\times\mathbf{r}] \tag{19}$$
$$= \frac{\omega_n}{2\pi}\frac{e}{4\pi r_n^2} N'[\delta(r-r_n)]\left(P_\ell^m(\cos\theta)\cos\left(m\phi+\omega_n' t\right)\right)\sin\theta\hat{\phi}$$

where to keep the form of the spherical harmonic as a traveling wave about the z-axis, $\omega_n' = m\omega_n$ and N and N' are normalization constants. The vectors are defined as

$$\hat{\phi} = \frac{\hat{u}\times\hat{r}}{|\hat{u}\times\hat{r}|} = \frac{\hat{u}\times\hat{r}}{\sin\theta}; \qquad \hat{u} = \hat{z} = \textit{orbital axis} \tag{20}$$

$$\hat{\theta} = \hat{\phi}\times\hat{r} \tag{21}$$

"^" denotes the unit vectors $\hat{u} \equiv \frac{\mathbf{u}}{|\mathbf{u}|}$, non-unit vectors are designed in bold, and the current function is normalized. For the electron source current given by Eq. (19), each comprising a multipole of order (ℓ,m) with a time dependence $e^{i\omega_n t}$, the far-field solutions to Maxwell's equations are given by

$$\mathbf{B} = -\frac{i}{k}a_M(\ell,m)\nabla\times g_\ell(kr)\mathbf{X}_{\ell.m}$$
$$\mathbf{E} = a_M(\ell,m)g_\ell(kr)\mathbf{X}_{\ell.m} \tag{22}$$

and the time-averaged power radiated per solid angle $\frac{dP(\ell,m)}{d\Omega}$ is

$$\frac{dP(\ell,m)}{d\Omega} = \frac{c}{8\pi k^2}\left|a_M(\ell,m)\right|^2\left|\mathbf{X}_{\ell.m}\right|^2 \tag{23}$$

where $a_M(\ell,m)$ is

$$a_M(\ell,m) = \frac{-ek^2}{c\sqrt{\ell(\ell+1)}}\frac{\omega_n}{2\pi}Nj_\ell(kr_n)\Theta\sin(mks) \tag{24}$$

In the case that k is the lightlike k^0, then $k = \omega_n / c$, in Eq. (24), and Eqs. (22-23) vanishes for

$$s = vT_n = R = r_n = \lambda_n \tag{25}$$

There is no radiation.

E. Magnetic Field Equations of the Electron

The orbitsphere is a shell of negative charge current comprising correlated charge motion along great circles. For $\ell = 0$, the orbitsphere gives rise to a magnetic moment of 1 Bohr magneton [45]. (The details of the derivation of the magnetic parameters including the electron g factor are given in Ref. [3] and Chp. 1 of Ref. [7].)

$$\mu_B = \frac{e\hbar}{2m_e} = 9.274\ X\ 10^{-24}\ JT^{-1} \tag{26}$$

The magnetic field of the electron shown in Figure 11 is given by

$$\mathbf{H} = \frac{e\hbar}{m_e r_n^3}(\mathbf{i}_r \cos\theta - \mathbf{i}_\theta \sin\theta) \qquad \text{for } r < r_n \tag{27}$$

$$\mathbf{H} = \frac{e\hbar}{2m_e r^3}(\mathbf{i}_r 2\cos\theta + \mathbf{i}_\theta \sin\theta) \qquad \text{for } r > r_n \tag{28}$$

The energy stored in the magnetic field of the electron is

$$E_{mag} = \frac{1}{2}\mu_o \int_0^{2\pi}\int_0^{\pi}\int_0^{\infty} H^2 r^2 \sin\theta dr d\theta d\Phi \tag{29}$$

$$E_{mag\ \text{total}} = \frac{\pi\mu_o e^2\hbar^2}{m_e^2 r_1^3} = \frac{4\pi\mu_o\mu_B^2}{r_1^3} \tag{30}$$

F. Stern-Gerlach Experiment

The Stern-Gerlach experiment implies a magnetic moment of one Bohr magneton and an associated angular momentum quantum number of 1/2. Historically, this quantum number is

called the spin quantum number, s ($s = \frac{1}{2}$; $m_s = \pm\frac{1}{2}$). The superposition of the vector projection of the orbitsphere angular momentum on the z-axis is $\frac{\hbar}{2}$ with an orthogonal component of $\frac{\hbar}{4}$. Excitation of a resonant Larmor precession gives rise to $\hbar$ on an axis **S** that precesses about the z-axis called the spin axis at the Larmor frequency at an angle of $\theta = \frac{\pi}{3}$ to give a perpendicular projection of

$$\mathbf{S}_{\perp} = \hbar \sin\frac{\pi}{3} = \pm\sqrt{\frac{3}{4}}\hbar\, \mathbf{i}_{Y_R} \tag{31}$$

and a projection onto the axis of the applied magnetic field of

$$\mathbf{S}_{\parallel} = \hbar \cos\frac{\pi}{3} = \pm\frac{\hbar}{2}\mathbf{i}_z \tag{32}$$

The superposition of the $\frac{\hbar}{2}$, z-axis component of the orbitsphere angular momentum and the $\frac{\hbar}{2}$, z-axis component of **S** gives $\hbar$ corresponding to the observed electron magnetic moment of a Bohr magneton, μ_B.

G. Electron g Factor

As given in the Electron g Factor section of Ref. [7] and Ref. [3], conservation of angular momentum of the orbitsphere permits a discrete change of its "kinetic angular momentum" ($\mathbf{r} \times m\mathbf{v}$) by the applied magnetic field of $\frac{\hbar}{2}$, and concomitantly the "potential angular momentum" ($\mathbf{r} \times e\mathbf{A}$) must change by $-\frac{\hbar}{2}$.

$$\Delta\mathbf{L} = \frac{\hbar}{2} - \mathbf{r} \times e\mathbf{A} \tag{33}$$

$$= \left[\frac{\hbar}{2} - \frac{e\phi}{2\pi}\right]\hat{z} \tag{34}$$

In order that the change of angular momentum, $\Delta\mathbf{L}$, equals zero, ϕ must be $\Phi_0 = \frac{h}{2e}$, the magnetic flux quantum. The magnetic moment of the electron is parallel or antiparallel to the applied field only. During the spin-flip transition, power must be conserved. Power flow is governed by the Poynting power theorem,

$$\nabla \bullet (\mathbf{E} \times \mathbf{H}) = -\frac{\partial}{\partial t}\left[\frac{1}{2}\mu_o \mathbf{H} \bullet \mathbf{H}\right] - \frac{\partial}{\partial t}\left[\frac{1}{2}\varepsilon_o \mathbf{E} \bullet \mathbf{E}\right] - \mathbf{J} \bullet \mathbf{E} \tag{35}$$

Eq. (36) gives the total energy of the flip transition which is the sum of the energy of reorientation of the magnetic moment (1st term), the magnetic energy (2nd term), the electric energy (3rd term), and the dissipated energy of a fluxon treading the orbitsphere (4th term), respectively,

$$\Delta E_{mag}^{spin} = 2\left(1 + \frac{\alpha}{2\pi} + \frac{2}{3}\alpha^2\left(\frac{\alpha}{2\pi}\right) - \frac{4}{3}\left(\frac{\alpha}{2\pi}\right)^2\right)\mu_B B \tag{36}$$

$$\Delta E_{mag}^{spin} = g\mu_B B \tag{37}$$

where the stored magnetic energy corresponding to the $\frac{\partial}{\partial t}\left[\frac{1}{2}\mu_o \mathbf{H} \bullet \mathbf{H}\right]$ term increases, the stored electric energy corresponding to the $\frac{\partial}{\partial t}\left[\frac{1}{2}\varepsilon_o \mathbf{E} \bullet \mathbf{E}\right]$ term increases, and the $\mathbf{J} \bullet \mathbf{E}$ term is dissipative. The spin-flip transition can be considered as involving a magnetic moment of g times that of a Bohr magneton.

The magnetic moment, m, of Eq. (36) is twice that from the gyromagnetic ratio as given by

$$m = \frac{\text{charge} \cdot \text{angular momentum}}{2 \cdot \text{mass}} \tag{38}$$

The magnetic moment of the electron is the sum of the component corresponding to the kinetic angular momentum, $\frac{\hbar}{2}$, and the component corresponding to the vector potential angular momentum, $\frac{\hbar}{2}$, (Eq. (33). The spin-flip transition can be considered as involving a magnetic moment of g times that of a Bohr magneton. The g factor is redesignated the fluxon g factor as opposed to the anomalous g factor, and it is given by Eq. (36).

$$\frac{g}{2} = 1 + \frac{\alpha}{2\pi} + \frac{2}{3}\alpha^2\left(\frac{\alpha}{2\pi}\right) - \frac{4}{3}\left(\frac{\alpha}{2\pi}\right)^2 \tag{39}$$

For $\alpha^{-1} = 137.03604(11)$ [46]

$$\frac{g}{2} = 1.001\ \ 159\ \ 652\ \ 120 \tag{40}$$

The experimental value [47] is

$$\frac{g}{2} = 1.001\ \ 159\ \ 652\ \ 188(4) \tag{41}$$

The calculated and experimental values are within the propagated error of the fine structure constant. Different values of the fine structure constant have been recorded from different experimental techniques, and α^{-1} depends on a circular argument between theory and experiment [32]. One measurement of the fine structure constant based on the electron g factor is $\alpha_{g_e}^{-1} = 137.036006(20)$ [35]. This value can be contrasted with equally precise measurements employing solid state techniques such as those based on the Josephson effect [48] ($\alpha_J^{-1} = 137.035963(15)$) or the quantized Hall effect [49] ($\alpha_H^{-1} = 137.035300(400)$). A method of the determination of α^{-1} that depends on the circular methodology between theory and experiment to a lesser extent is the substitution of the independently measured fundamental

constants μ_0, e, c, and h into Eq. (71). The following values of the fundamental constants are given by Weast [46]

$$\mu_o = 4\pi X 10^{-7} Hm^{-1} \tag{42}$$

$$e = 1.6021892(46)\ X\ 10^{-19}\ C \tag{43}$$

$$c = 2.99792458(12)\ X 10^{8}\ ms^{-1} \tag{44}$$

$$h = 6.626176(36)\ X\ 10^{-34}\ JHz^{-1} \tag{45}$$

For these constants,

$$\alpha^{-1} = 137.03603(82) \tag{46}$$

Substitution of the α^{-1} from Eq. (46) into Eq. (39) gives

$$\frac{g}{2} = 1.001\ \ 159\ \ 652\ \ 137 \tag{47}$$

The experimental value [47] is

$$\frac{g}{2} = 1.001\ \ 159\ \ 652\ \ 188(4) \tag{48}$$

The *postulated* QED theory of $\frac{g}{2}$ is based on the determination of the terms of a *postulated* power series in α/π where each *postulated* virtual particle is a source of *postulated* vacuum polarization that gives rise to a *postulated* term. The algorithm involves scores of *postulated* Feynman diagrams corresponding to thousands of matrices with thousands of integrations per matrix requiring decades to reach a consensus on the "appropriate" *postulated* algorithm to remove the intrinsic infinities. The remarkable agreement between Eqs. (47) and (48) demonstrates that $\frac{g}{2}$ may be derived in closed form from Maxwell's equations in a simple straightforward manner that yields a result with eleven figure agreement with experiment—the limit of the experimental capability of the measurement of α directly or the fundamental constants to determine α. In Sec. II and Chp. 1, Appendix II of Ref. [7], the Maxwellian result is contrasted with the QED algorithm of invoking virtual particles, zero point fluctuations of the vacuum, and negative energy states of the vacuum. Rather than an infinity of radically different QED models, an essential feature is that *Maxwellian solutions are unique*.

H. Spin and Orbital Parameters

The total function that describes the spinning motion of each electron orbitsphere is composed of two functions. One function, the spin function, is spatially uniform over the orbitsphere, spins with a quantized angular velocity, and gives rise to spin angular momentum. The other function, the modulation function, can be spatially uniform—in which case there is no orbital angular momentum and the magnetic moment of the electron orbitsphere is one Bohr magneton—or not spatially uniform—in which case there is orbital angular momentum. The modulation function also rotates with a quantized angular velocity.

The spin function of the electron corresponds to the nonradiative $n = 1$, $\ell = 0$ state of atomic hydrogen which is well known as an s state or orbital. (See Figure 1 for the charge function and Figure 2 for the current function.) In cases of orbitals of heavier elements and excited states of one electron atoms and atoms or ions of heavier elements with the ℓ quantum number not equal to zero and which are not constant as given by Eq. (14), the constant spin function is modulated by a time and spherical harmonic function as given by Eq. (15) and shown in Figure 3. The modulation or traveling charge density wave corresponds to an orbital angular momentum in addition to a spin angular momentum. These states are typically referred to as p, d, f, etc. orbitals. Application of Haus's [39] condition also predicts nonradiation for a constant spin function modulated by a time and spherically harmonic orbital function. There is acceleration without radiation as also shown in Sec. IIIDc. (Also see Abbott and Griffiths, Goedecke, and Daboul and Jensen [42-44]). However, in the case that such a state arises as an excited state by photon absorption, it is radiative due to a radial dipole term in its current density function since it possesses spacetime Fourier Transform components synchronous with waves traveling at the speed of light [39]. (See Instability of Excited States section of Ref. [7].)

a. Moment of Inertia and Spin and Rotational Energies

The moments of inertia and the rotational energies as a function of the ℓ quantum number for the solutions of the time-dependent electron charge density functions (Eqs. (14-15)) given in Sec. IIIC are solved using the rigid rotor equation [41]. The details of the derivations of the results as well as the demonstration that Eqs. (14-15) with the results given *infra.* are solutions of the wave equation are given in Chp 1, Rotational Parameters of the Electron (Angular Momentum, Rotational Energy, Moment of Inertia) section of Ref. [7].

$\ell = 0$

$$I_z = I_{spin} = \frac{m_e r_n^{\,2}}{2} \tag{49}$$

$$L_z = I\omega \mathbf{i}_z = \pm\frac{\hbar}{2} \tag{50}$$

$$E_{rotational} = E_{rotational,\,spin} = \frac{1}{2}\left[I_{spin}\left(\frac{\hbar}{m_e r_n^{\,2}}\right)^2 \right] = \frac{1}{2}\left[\frac{m_e r_n^{\,2}}{2}\left(\frac{\hbar}{m_e r_n^{\,2}}\right)^2 \right] = \frac{1}{4}\left[\frac{\hbar^2}{2I_{spin}} \right] \tag{51}$$

$$T = \frac{\hbar^2}{2m_e r_n^2} \tag{52}$$

$\ell \neq 0$

$$I_{orbital} = m_e r_n^{\,2}\left[\frac{\ell(\ell+1)}{\ell^2 + 2\ell + 1} \right]^{\frac{1}{2}} = m_e r_n^{\,2}\sqrt{\frac{\ell}{\ell+1}} \tag{53}$$

$$\mathbf{L} = I\omega\mathbf{i}_z = I_{orbital}\omega\mathbf{i}_z = m_e r_n^{\,2}\left[\frac{\ell(\ell+1)}{\ell^2 + 2\ell + 1} \right]^{\frac{1}{2}}\omega\mathbf{i}_z = m_e r_n^{\,2}\frac{\hbar}{m_e r_n^{\,2}}\sqrt{\frac{\ell}{\ell+1}} = \hbar\sqrt{\frac{\ell}{\ell+1}} \tag{54}$$

$$L_{z\ total} = L_{z\,spin} + L_{z\,orbital} \tag{55}$$

$$E_{rotational\ \text{orbital}} = \frac{\hbar^2}{2I}\left[\frac{\ell(\ell+1)}{\ell^2 + 2\ell + 1} \right] = \frac{\hbar^2}{2I}\left[\frac{\ell}{\ell+1} \right] = \frac{\hbar^2}{2m_e r_n^{\,2}}\left[\frac{\ell}{\ell+1} \right] \tag{56}$$

$$\left\langle L_{z\,orbital} \right\rangle = 0 \tag{57}$$

$$\left\langle E_{rotational\ \text{orbital}} \right\rangle = 0 \tag{58}$$

The orbital rotational energy arises from a spin function (spin angular momentum) modulated by a spherical harmonic angular function (orbital angular momentum). The time-averaged

mechanical angular momentum and rotational energy associated with the wave-equation solution comprising a traveling charge-density wave on the orbitsphere is zero as given in Eqs. (57) and (58), respectively. Thus, the principal levels are degenerate except when a magnetic field is applied. In the case of an excited state, the angular momentum of $\hbar$ is carried by the fields of the trapped photon. The amplitudes that couple to external magnetic and electromagnetic fields are given by Eq. (54) and (56), respectively. The rotational energy due to spin is given by Eq. (51), and the total kinetic energy is given by Eq. (52).

I. Force Balance Equation

The radius of the nonradiative ($n = 1$) state is solved using the electromagnetic force equations of Maxwell relating the charge and mass density functions wherein the angular momentum of the electron is given by $\hbar$ [7]. The reduced mass arises naturally from an electrodynamic interaction between the electron and the proton of mass m_p.

$$\frac{m_e}{4\pi r_1^2}\frac{v_1^2}{r_1} = \frac{e}{4\pi r_1^2}\frac{Ze}{4\pi\varepsilon_o r_1^2} - \frac{1}{4\pi r_1^2}\frac{\hbar^2}{m_p r_n^3} \tag{59}$$

$$r_1 = \frac{a_H}{Z} \tag{60}$$

where a_H is the radius of the hydrogen atom.

J. Energy Calculations

From Maxwell's equations, the potential energy V, kinetic energy T, electric energy or binding energy E_{ele} are

$$V = \frac{-Ze^2}{4\pi\varepsilon_o r_1} = \frac{-Z^2e^2}{4\pi\varepsilon_o a_H} = -Z^2\ X\ 4.3675\ X\ 10^{-18}\ J = -Z^2\ X\ 27.2\ eV \tag{61}$$

$$T = \frac{Z^2 e^2}{8\pi\varepsilon_o a_H} = Z^2 \, X \, 13.59 \; eV \tag{62}$$

$$T = E_{ele} = -\frac{1}{2}\varepsilon_o \int_{\infty}^{r_1} \mathbf{E}^2 dv \quad \text{where } \mathbf{E} = -\frac{Ze}{4\pi\varepsilon_o r^2} \tag{63}$$

$$E_{ele} = -\frac{Ze^2}{8\pi\varepsilon_o r_1} = -\frac{Z^2 e^2}{8\pi\varepsilon_o a_H} = -Z^2 \, X \, 2.1786 \, X \, 10^{-18} \; J = -Z^2 \, X \, 13.598 \; eV \tag{64}$$

The calculated Rydberg constant is $10,967,758\, m^{-1}$; the experimental Rydberg constant is $10,967,758\, m^{-1}$. For increasing Z, the velocity becomes a significant fraction of the speed of light; thus, special relativistic corrections were included in the calculation of the ionization energies of one-electron atoms that are given in Table 1.

K. Resonant Line Shape and Lamb Shift

The spectroscopic linewidth arises from the classical rise-time band-width relationship, and the Lamb Shift is due to conservation of energy and linear momentum and arises from the radiation reaction force between the electron and the photon. It follows from the Poynting Power Theorem (Eq. (35)) with spherical radiation that the transition probabilities are given by the ratio of power and the energy of the transition [52]. The hydrogen electric dipole transition probability due to the transient radial current from the initial quantum state n_i, ℓ, m_ℓ, m_s and radius r_{n_i} to the final $n_i, \ell \pm 1, m_\ell, m_s$ and radius r_{n_f} derived in Ref. [7] is

$$\frac{1}{\tau} = \frac{power}{energy} \tag{65}$$

$$\begin{aligned} \frac{1}{\tau} &= \frac{1}{m_e c^2} \frac{\eta}{24\pi} \left(\frac{e\hbar}{m_e a_0^2} \right)^2 \frac{1}{\left(n_f n_i \right)^2} \\ &= 2.678 \; X \; 10^9 \frac{1}{\left(n_f n_i \right)^2} \, s^{-1} \end{aligned} \tag{67}$$

This rise-time gives rise to Γ, the spectroscopic line-width. The relationship between the rise-time and the band-width is given by Siebert [53].

$$\tau^2 = 4\left[\frac{\int_{-\infty}^{\infty} t^2 h^2(t)dt}{\int_{-\infty}^{\infty} h^2(t)dt} - \left(\frac{\int_{-\infty}^{\infty} t h^2(t)dt}{\int_{-\infty}^{\infty} h^2(t)dt}\right)^2\right] \tag{67}$$

$$\Gamma^2 = 4\frac{\int_{-\infty}^{\infty} f^2 |H(f)|^2 df}{\int_{-\infty}^{\infty} |H(f)|^2 df} \tag{68}$$

By application of the Schwartz inequality, the relationship between the rise-time and the band-width is[3]

$$\tau\Gamma \geq \frac{1}{\pi} \tag{69}$$

From Eq. (66), the line-width is proportional to the ratio of the Quantum Hall resistance, $\frac{h}{e^2}$,

---

[3] Eq.(69) is erroneously interpreted as a physical law of the indeterminate nature of conjugate parameters of atomic particles such as position and momentum or energy and time. This so called Heisenberg Uncertainty Principle is not a physical law, rather it is a misinterpretation of applying the Schwartz Inequality to a probability-wave model of a particle [54]. The mathematical consequence is that the particle such as an electron can have a continuum of momenta and positions with a continuum of energies simultaneously which can not be physical. This result is independent of error or limitations introduced by measurement. Jean B. Fourier was the first to discovery the relationship between time and frequency compositions of physical measurables. Eq. (69) expresses the limitation of measuring these quantities since an impulse contains an infinity of frequencies, and no instrument has such bandwidth. Similarly, an exact frequency requires and infinite measurement time, and all measurements must be finite in length. Thus, Eq. (69) is a statement about the limitations of measurement in time and frequency. It is further a conservation statement of energy of a signal in the time and frequency domains. Werner Heisenberg's substitution of momentum and position for a single particle, probability-wave into this relationship says nothing about conjugate parameters of a particle in the absence of their measurement or the validity of the probability-wave model. In fact, this approach has been shown to be flawed experimentally as shown in the Wave-Particle Duality section, Appendix II: Quantum Electrodynamics (QED) is Purely Mathematical and Has No Basis

and, η, the radiation resistance of free space.

$$\eta = \sqrt{\frac{\mu_0}{\varepsilon_0}} \tag{70}$$

And, the Quantum Hall resistance given in the Quantum Hall Effect section of Ref. [7] was derived using the Poynting Power Theorem. Also, from Eq. (66), the line-width is proportional to the fine structure constant, α,

$$\alpha = \frac{1}{4\pi}\sqrt{\frac{\mu_0}{\varepsilon_0}}\frac{e^2}{\hbar} = \frac{1}{2}\frac{\sqrt{\frac{\mu_0}{\varepsilon_0}}}{\frac{h}{e^2}} = \frac{\mu_0 e^2 c}{2h} \tag{71}$$

During a transition, the total energy of the system decays exponentially. Applying Eqs. (67) and (68) to the case of exponential decay,

$$h(t) = e^{-\alpha t}u(t) = e^{-\frac{2\pi}{T}t}u(t) \tag{72}$$

$$|H(f)| = \frac{1}{\sqrt{\left(\frac{1}{T}\right)^2 + (2\pi f)^2}} \tag{73}$$

where the rise-time, τ, is the time required for $h(t)$ of Eq. (72) to decay to $1/e$ of its initial value and where the band-width, Γ, is the half-power bandwidth, the distance between points at which

$$|H(f)| = \frac{|H(0)|}{\sqrt{2}} \tag{74}$$

From Eq. (67) [53],

$$\tau = T \tag{75}$$

From Eq. (68) [53],

---

in Reality of Ref. [7] and discussed previously [2, 9-10].

$$\Gamma = \frac{1}{\pi T} \tag{76}$$

From Eq. (75) and Eq. (76), the relationship between the rise-time and the band-width for exponential decay is

$$\tau\Gamma = \frac{1}{\pi} \tag{77}$$

Photons obey Maxwell-Boltzmann statistics. The emitted radiation, the summation of an ensemble of emitted photons each of an exact frequency and energy given by Eq. (87), appears as a wave train with effective length c/Γ. Such a finite pulse of radiation is not exactly monochromatic but has a frequency spectrum covering an interval of the order Γ. The exact shape of the frequency spectrum is given by the square of the Fourier transform of the electric field. Thus, the amplitude spectrum is proportional to

$$\mathbf{E}(\omega) \propto \int_0^\infty e^{-\alpha_t t} e^{-i\omega t} dt = \frac{1}{\alpha_t - i\omega} \tag{78}$$

The coefficient α_t corresponds to the spectroscopic linewidth and also to a shift in frequency that arises from the radiation reaction force between the electron and the photon. The energy radiated per unit frequency interval is therefore

$$\frac{dI(\omega)}{d\omega} = I_0 \frac{\Gamma}{2\pi} \frac{1}{\left(\omega - \omega_0 - \Delta\omega\right)^2 + \left(\Gamma/2\right)^2} \tag{79}$$

where I_0 is the total energy radiated. The spectral distribution is called a resonant line shape. The width of the distribution at half-maximum intensity is called the half-width or line-breadth and is equal to Γ. Shown in Figure 12 is such a spectral line. Because of the reactive effects of radiation the line is shifted in frequency. The small radiative shift of the energy levels of atoms was first observed by Lamb in 1947 [24] and is called the Lamb Shift in his honor.

The Lamb Shift of the ${}^2P_{1/2}$ state of the hydrogen atom having the quantum number $\ell = 1$ is calculated by applying conservation of energy and linear momentum to the emitted photon, electron, and atom. The photon emitted by an excited state atom carries away energy, linear momentum, and angular momentum. The initial and final values of the energies and momenta must be conserved between the atom, the electron, and the photon. (Conservation of angular momentum is used to derive the photon's equation in the Equation of the Photon section of Ref. [7]). Consider an isolated atom of mass M having an electron of mass m_e in an excited state level at an energy E and moving with velocity $\mathbf{V}$ along the direction in which the photon is to be emitted (the components of motion perpendicular to this direction remain unaffected by the emission and may be ignored). The energy above the "ground" state at rest is

$$\left(E + \frac{1}{2} M\mathbf{V}^2\right) \tag{80}$$

When a photon of energy $E_{h\upsilon}$ is emitted, the atom and/or electron recoils and has a new velocity

$$\mathbf{V} + \mathbf{v} \tag{81}$$

(which is a vector sum in that $\mathbf{V}$ and $\mathbf{v}$ may be opposed), and a total energy of

$$\frac{1}{2} M(\mathbf{V} + \mathbf{v})^2 \tag{82}$$

By conservation of energy,

$$E + \frac{1}{2} M\mathbf{V}^2 = E_{h\upsilon} + \frac{1}{2} M(\mathbf{V} + \mathbf{v})^2 \tag{83}$$

so, that the actual energy of the photon emitted is given by

$$\begin{aligned} E_{h\upsilon} &= E - \frac{1}{2} M\mathbf{v}^2 - M\mathbf{v}\mathbf{V} \\ E_{h\upsilon} &= E - E_R - E_D \end{aligned} \tag{84}$$

The photon is thus deficient in energy by a recoil kinetic energy

$$E_R = \frac{1}{2} M\mathbf{v}^2 \tag{85}$$

which is independent of the initial velocity $\mathbf{V}$, and by a thermal or Doppler energy

$$E_D = M\mathbf{v}\mathbf{V} \tag{86}$$

which depends on $\mathbf{V}$; therefore, it can be positive or negative.

Momentum must also be conserved in the emission process. The energy, E, of the photon is given by Planck's equation:

$$E = \hbar\omega = h\frac{\omega}{2\pi} = h\nu = hf = h\frac{c}{\lambda} \tag{87}$$

From special relativity,

$$E = \hbar\omega = mc^2 \tag{88}$$

Thus, $\mathbf{p}$, the momentum of the photon is

$$\mathbf{p} = mc = \frac{E_{h\nu}}{c} \tag{89}$$

where c is the velocity of light, so that

$$M\mathbf{V} = M(\mathbf{V} + \mathbf{v}) + \frac{E_{h\nu}}{c} \tag{90}$$

And, the recoil momentum is

$$M\mathbf{v} = -\frac{E_{h\nu}}{c} \tag{91}$$

Thus, the recoil energy is given by

$$E_R = \frac{E_{h\nu}^2}{2Mc^2} \tag{92}$$

and depends on the mass of the electron and/or atom and the energy of the photon. The Doppler energy, E_D, is dependent on the thermal motion of the atom, and will have a distribution of values which is temperature dependent. A mean value, E_D, can be defined which is related to

the mean kinetic energy per translational degree of freedom [55-56]

$$\bar{E}_D \cong \frac{1}{2} kT \tag{93}$$

by

$$\bar{\bar{E}}_D \cong 2\sqrt{E_K E_R} = E_{h\nu}\sqrt{\frac{2\bar{\bar{E}}_K}{Mc^2}} \tag{94}$$

where k is Boltzmann's constant and T is the absolute temperature. As a result, the statistical distribution in energy of the emitted photons is displaced from the true excited-state energy by $-E_R$ and broadened by E_D into a Gaussian distribution of width $2\bar{E}_D$. The distribution for absorption has the same shape but is displaced by $+E_R$.

For the transition of the hydrogen atom with $n = 2$ and $\ell = 0$ in the initial and final states, the emitted angular radiation power pattern is uniform. The linear momentum of the photon is balanced by the recoil momentum of the entire atom of mass m_H. The recoil frequency of the hydrogen atom, Δf, is given by combining Eqs. (87) and (92).

$$\Delta f = \frac{\Delta\omega}{2\pi} = \frac{E_{h\upsilon}}{h} = \frac{\left(E_{h\upsilon}\right)^2}{2hm_H c^2} = 13.3952\ MHz \tag{95}$$

where $E_{h\upsilon}$ corresponding to the recoil energy (Eq. (92)) is

$$\begin{aligned} &E_{h\nu} = 13.5983\ eV\left(1 - \frac{1}{n^2}\right) - h\Delta f\ ; \qquad h\Delta f <<< 10\ eV; \qquad n = 2 \\ &\therefore E_{h\nu} = 13.5983\ eV\left(1 - \frac{1}{n^2}\right) \end{aligned} \tag{96}$$

However, during the emission of a photon by an excited state atom with $\ell \neq 0$, the angular radiation power pattern is not uniform because the charge density of the electron is not uniform. With $\ell \neq 0$, the charge-density function is a constant function plus a spherical harmonic function (angular modulation) corresponding to spin and orbital angular momenta, respectively, as given

in Secs. IIIC and IIIH and the One-Electron Atom section of Ref. [7]. In the case of $\ell = 1$ $m_\ell = 0$ designated the p_x orbital, the angular charge-density function is

$$\rho(r,\theta,\phi,t) = \frac{e}{4\pi r^2}[\delta(r - r_n)]\left[Y_0^0(\theta,\phi) + \mathrm{Re}\left\{Y_\ell^m(\theta,\phi)e^{i\omega_n t}\right\}\right] \tag{97}$$

where $\mathrm{Re}\left\{Y_\ell^m(\theta,\phi)e^{i\omega_n t}\right\} = P_\ell^m(\cos\theta)\cos(m\phi + \omega_n t)$ and $\omega_n = 0$ for $m = 0$.

$$Y_{1,z} = \cos\theta \tag{98}$$

Figure 3 gives pictorial representation of how the modulation function changes the electron density on the orbitsphere for several ℓ values. Consequently, rather than the electron recoiling as a point at the origin with transfer of the momentum to the nucleus such that the recoil is with the atom, the electron recoils independently of the atom, and it receives the majority of the recoil momentum according to Eq. (92) since the electron mass is 1/1836 times that of the nucleus. The conservation of the momentum between the electron and the photon depends of the angular distribution of the charge density relative to the photon linear propagation axis. Thus, the solid angle must be considered. As given in the Equation of the Photon section of Ref. [7] the angular momentum, $\mathbf{m}$, from the time-averaged angular-momentum density of the emitted photon is given by Eq. (16.61) of Jackson [57] in cgs units:

$$\mathbf{m} = \int \frac{1}{8\pi c}\mathrm{Re}[\mathbf{r} \times (\mathbf{E} \times \mathbf{B}^*)]dx^4 = \hbar \tag{99}$$

where the energy, E, is given from the Poynting power density [58]:

$$E = \int \frac{c}{4\pi}\mathrm{Re}(\mathbf{E} \times H^*)dx^4 = \hbar\omega \tag{100}$$

Since the fields have the same multipolarity as the source, from Eqs. (99-100), the radiation power pattern depends on the integral of the angular function squared, $\left(Y_\ell^m(\theta,\phi)\right)^2$. Specifically, the radiation power pattern of the electron in the ${}^2P_{1/2}$ ($\ell = 1$; $m_\ell = 0$) state follows from the

integral of the square of Eq. (98) over the spherical solid angle as given by McQuarrie [41]:

$$\int_0^{2\pi}\int_0^{\pi}\left(Y_1^0(\theta,\phi)\right)^2 \sin\theta d\theta d\phi = \frac{4\pi}{3} \tag{101}$$

The inverse of Eq. (101) is the weighting factor of momentum transfer due to the radiation power pattern as given for antennas after Kong [59].

The spherical and time harmonics, $\mathrm{Re}\left\{Y_\ell^m(\theta,\phi)e^{i\omega_n t}\right\}$, of the p_x orbital and ${}^2P_{1/2}$ state correspond to a constant current about the z-axis. In this case, the photon-momentum transfer for the ${}^2P_{1/2}\rightarrow{}^2S_{1/2}$ transition causes an excitation of a Larmor precession of a vector **S** having $\hbar$ of angular momentum about the z-axis at an angle of $\theta=\frac{\pi}{3}$ as given in the Spin Angular Momentum of the Orbitsphere with $\ell = 0$ section of Ref. [7]. In this case, the orbital angular momentum (Eq. (2.27) of Ref. [7]) is zero before and after the transition, and the invariance of each of $\frac{e}{m_e}$ of the electron, the electron angular momentum of $\hbar$, and the electron magnetic moment of μ_B from the spin angular momentum is maintained. From Eq. (1.74a) of Ref. [7], the projection of **S** onto the transverse plane (xy-plane) is $\mathbf{S}_\perp = \hbar\sin\frac{\pi}{3} = \pm\sqrt{\frac{3}{4}}\hbar\,\mathbf{i}_{Y_R}$. Then, the photon energy is corrected by the factor $\sqrt{\frac{3}{4}}$ due to electron recoil from the emission of a photon from the ${}^2P_{1/2}$ state corresponding to the rotating transverse component of momentum transfer. In this case, $E_{h\upsilon}$ corresponding to the recoil energy (Eq. (92)) including the factor from Eq. (101) is

$$E_{h\nu} = 13.5983\ eV\left(1-\frac{1}{n^2}\right)\frac{3}{4\pi}\sqrt{\frac{3}{4}} - h\Delta f$$
$$h\Delta f <<< 10\ eV;\quad n = 2 \tag{102}$$
$$\therefore E_{h\nu} = 13.5983\ eV\left(1-\frac{1}{2^2}\right)\frac{3}{4\pi}\sqrt{\frac{3}{4}}$$

The electron contribution to the Lamb Shift of the ${}^2P_{1/2}$ state of the hydrogen atom relative to the higher energy state ${}^2S_{1/2}$ is given by combining Eqs. (87), (92), (101), and (102):

$$\Delta f = \frac{\Delta\omega}{2\pi} = \frac{E_{h\upsilon}}{h} = \frac{\left(E_{h\upsilon}\right)^2}{2h\mu_e c^2} = 1052.48\ MHz \tag{103}$$

wherein the reduced mass of the electron given by Eq. (1.224) of Ref. [7] corrects for the finite mass of the nucleus during excitation of the precession of **S** [60]. Furthermore, since **S** rotates about the z-axis at $\theta = \frac{\pi}{3}$, it has a static projection of the angular momentum of $\mathbf{S}_{\|} = \pm\hbar\cos\frac{\pi}{3} = \pm\frac{\hbar}{2}\ \mathbf{i}_{Z_R}$ as given by Eq. (1.74b) of Ref. [7]. The energy and angular momentum of the photon correspond according to Eqs. (89) and (99-100). Therefore, the recoil energy of the photon corresponding to momentum transfer to the atom along the z-axis for the ${}^2P_{1/2}$ transition is given by the sum of the atom-alone term given by Eq. (95) and that due to $\mathbf{S}_{\|}$, minus the electron recoil term corresponding to $\mathbf{S}_{\perp}$:

$$\Delta f = \frac{\Delta\omega}{2\pi} = \frac{E_{h\upsilon}}{h} = \frac{\left(E_{h\upsilon}\right)^2}{2hm_H c^2} = \frac{\left(13.5983\ eV\left(1-\frac{1}{2^2}\right)\left(1+\frac{1}{2}-\sqrt{\frac{3}{4}}\right)\right)^2}{2hm_H c^2} = 5.3839\ MHz \tag{104}$$

Momentum of the electron, atom, and photon are conserved. The total recoil energy is the sum of the electron component (Eq. (103)) and the atom component (Eq. (104)). Thus, the calculated Lamb Shift due to both components of momentum transfer is

$$\Delta f = 1052.48\ MHz + 5.3839\ MHz = 1057.87\ MHz \tag{105}$$

The experimental Lamb Shift is $\Delta f = 1057.862\ MHz$ [61].

L. Spin-Orbital Coupling (Fine Structure)

The electron's motion in the hydrogen atom is always perpendicular to its radius; consequently, as shown by Eq. (7), the electron's angular momentum of $\hbar$ is invariant. Furthermore, the electron is nonradiative due to its angular motion as shown in Sec. IIID. The radiative instability of excited states is due to a radial dipole term in the function representative of the excited state due to the interaction of the photon and the excited state electron as shown in the Instability of Excited States section of Ref. [7]. The angular momentum of the photon given in the Equation of the Photon section of Ref. [7] is $\mathbf{m} = \int \frac{1}{8\pi c} \mathrm{Re}[\mathbf{r} \times (\mathbf{E} \times \mathbf{B}^*)] dx^4 = \hbar$. It is conserved for the solutions for the resonant photons and excited state electron functions given in the Excited States of the One-Electron Atom (Quantization) section and the Equation of the Photon section of Ref. [7]. Thus, the electrodynamic angular momentum and the inertial angular momentum are matched such that the correspondence principle holds. It follows from the principle of conservation of angular momentum that $\frac{e}{m_e}$ of the Bohr magneton (Eq. (26)) is invariant (See the Determination of Orbitsphere Radii r_n section of Ref. [7]).

A magnetic field is a relativistic effect of the electrical field as shown by Jackson [62]. No energy term is associated with the magnetic field of the electron of the hydrogen atom unless another source of magnetic field is present. In the case of spin-orbital coupling, the invariant $\hbar$ of spin angular momentum and orbital angular momentum each give rise to a corresponding invariant magnetic moment of a Bohr magneton, and their corresponding energies superimpose as given in the Orbital and Spin Splitting section of Ref. [7]. The interaction of the two magnetic

moments gives rise to a relativistic spin-orbital coupling energy. The vector orientations of the momenta must be considered as well as the condition that flux must be linked by the electron in units of the magnetic flux quantum in order to conserve the invariant electron angular momentum of $\hbar$. The energy may be calculated with the additional conditions of the invariance of the electron's charge and mass to charge ratio $\frac{e}{m_e}$.

As shown in Sec. IIIG and the Electron g Factor section (Eq. (1.149) of Ref. [7] and second RHS term of Eq. (36)) of Ref. [7], flux must be linked by the electron orbitsphere in units of the magnetic flux quantum that treads the orbitsphere at $v = c$ with a corresponding energy of

$$E_{mag}^{fluxon} = 2\frac{\alpha}{2\pi}\mu_B B \tag{106}$$

As shown in the Orbitsphere Equation of Motion for $\ell = 0$ section of Ref. [7], the maximum projection of the rotating spin angular momentum of the electron onto an axis is $\sqrt{\frac{3}{4}}\hbar$. From Eq. (38), the magnetic flux due to the spin angular momentum of the electron is [45]

$$\mathbf{B} = \frac{\mu_0 \mu}{r^3} = \sqrt{\frac{3}{4}}\frac{\mu_0 e\hbar}{2m_e r_2^3} \tag{107}$$

where μ is the magnetic moment. The maximum projection of the orbital angular momentum onto an axis is $\hbar$ as shown in the Orbital and Spin Splitting section of Ref. [7] with a corresponding magnetic moment of a Bohr magneton μ_B. Substitution of the magnetic moment of μ_B corresponding to the orbital angular momentum and Eq. (107) for the magnetic flux corresponding to the spin angular momentum into Eq. (106) gives the spin-orbital coupling energy $E_{s/o}$.

$$E_{s/o} = 2\frac{\alpha}{2\pi}\mu_B B = 2\sqrt{\frac{3}{4}}\frac{\alpha}{2\pi}\left(\frac{e\hbar}{2m_e}\right)\frac{\mu_0 e\hbar}{2m_e r^3} \tag{108}$$

The Bohr magneton corresponding to the orbital angular momentum is invariant and the corresponding invariant electron charge e is common with that which gives rise to the magnetic field due to the spin angular momentum. The condition that the magnetic flux quantum treads the orbitsphere at $v = c$ with the maintenance of the invariance of the electron's mass to charge ratio $\frac{e}{m_e}$ and electron angular momentum of $\hbar$ requires that the radius and the electron mass of the magnetic field term of Eq. (108) be relativistically corrected. As shown in Sec. IIIDa, the Spacetime Fourier Transform of the Electron Function section, and the Determination of Orbitsphere Radii r_n section of Ref. [7], the relativistically corrected radius r^* follows from the relationship between the electron wavelength and the radius.

$$2\pi r = \lambda \tag{109}$$

As shown in the Excited States of the One-Electron Atom (Quantization) section of Ref. [7], the phase matching condition requires that the electron wavelength be the same for orbital and spin angular momentum. With $v = c$,

$$r^* = \lambda \tag{110}$$

Thus,

$$r^* = \frac{r}{2\pi} \tag{111}$$

The relativistically corrected mass m^* follows from Eq. (111) with maintenance of the invariance of the electron angular momentum of $\hbar$ given by Eqs. (6) and (7).

$$m\mathbf{r} \times \mathbf{v} = m_e r \frac{\hbar}{m_e r} \tag{112}$$

With Eq. (111), the relativistically corrected mass m^* is

$$m^* = 2\pi m_e \tag{113}$$

With the substitution of Eq. (111) and Eq. (113) into Eq. (108), the spin-orbital coupling energy $E_{s/o}$ is given by

$$E_{s/o} = 2\frac{\alpha}{2\pi}\left(\frac{e\hbar}{2m_e}\right)\frac{\mu_0 e\hbar}{2(2\pi m_e)\left(\frac{r}{2\pi}\right)^3}\sqrt{\frac{3}{4}} = \sqrt{\frac{3}{4}}\frac{\alpha\pi\mu_0 e^2\hbar^2}{m_e^2 r^3} \tag{114}$$

(The magnetic field in this case is equivalent to that of a point electron at the origin with $\sqrt{\frac{3}{4}}\hbar$ of angular momentum.)

In the case that $n = 2$, the radius given by Eq. (4) is $r = 2a_0$. The predicted energy difference between the ${}^2P_{3/2}$ and ${}^2P_{1/2}$ levels of the hydrogen atom, $E_{s/o}$, given by Eq. (114) is

$$E_{s/o} = \sqrt{\frac{3}{4}}\frac{\alpha\pi\mu_0 e^2\hbar^2}{8m_e^2 a_0^3} \tag{115}$$

wherein $\ell = 1$ and both levels are equivalently Lamb shifted.

$E_{s/o}$ may be expressed in terms of the mass energy of the electron. The energy stored in the magnetic field of the electron orbitsphere (Eq. (30)) is

$$E_{mag} = \frac{\pi\mu_o e^2\hbar^2}{(m_e)^2 r_n^3} \tag{116}$$

As shown in the Pair Production section of Ref. [7] with the $v = c$ condition, the result of the substitution of $\alpha a_o = \lambda\!\!\!^{-}_C$ for r_n, the relativistic mass, $2\pi m_e$, for m_e, and multiplication by the relativistic correction, α^{-1}, which arises from Gauss' law surface integral and the relativistic invariance of charge is

$$E_{mag} = m_e c^2 \tag{117}$$

Thus, Eq. (115) can be expressed as

$$E_{s/o} = \frac{\alpha^5 (2\pi)^2}{8} m_e c^2 \sqrt{\frac{3}{4}} \qquad (118)$$
$$= 4.51905\ X\ 10^{-5}\ eV$$

Using the Planck equation, the corresponding frequency, $\Delta f_{s/o}$, is

$$\Delta f_{s/o} = 10,927.0\ MHz \qquad (119)$$

As in the case of the ${}^2P_{1/2} \rightarrow {}^2S_{1/2}$ transition, the photon-momentum transfer for the ${}^2P_{3/2} \rightarrow {}^2P_{1/2}$ transition causes an excitation of a Larmor precession of a vector **S** having $\hbar$ of angular momentum about the z-axis at an angle of $\theta = \frac{\pi}{3}$ as given in the Spin Angular Momentum of the Orbitsphere with $\ell = 0$ section of Ref. [7]. In addition, $\Delta m_\ell = -1$; then, the photon energy is corrected by the factor $1 - \sqrt{\frac{3}{4}}$ due to electron recoil from the emission of a photon from the ${}^2P_{3/2}$ state corresponding to the rotating transverse component of momentum transfer. In this case, from Eq. (102), $E_{h\upsilon}$ is

$$E_{h\nu} = 13.5984\ eV\left(1 - \frac{1}{2^2}\right)\frac{3}{4\pi}\left(1 - \sqrt{\frac{3}{4}}\right) \qquad (120)$$
$$= 0.326196\ eV$$

The electron contribution to the recoil shift of the ${}^2P_{3/2} \rightarrow {}^2P_{1/2}$ transition given by Eqs. (103) and (120) is

$$\Delta f = \frac{\Delta\omega}{2\pi} = \frac{E_{h\upsilon}}{h} = \frac{(E_{h\upsilon})^2}{2h\mu_e c^2} = \frac{\left(13.5984\ eV\left(1 - \frac{1}{2^2}\right)\frac{3}{4\pi}\left(1 - \sqrt{\frac{3}{4}}\right)\right)^2}{2h\mu_e c^2} = 25.1883\ MHz \qquad (121)$$

Furthermore, $\Delta m_\ell = -1$ corresponds to the static angular momentum change of $\hbar\,\mathbf{i}_{Z_R}$. Therefore, from Eq. (104), the recoil energy of the photon corresponding to momentum transfer to the atom along the z-axis for the ${}^2P_{3/2} \rightarrow {}^2P_{1/2}$ transition due to the atom-alone term given by Eq. (95) and

that due to $\Delta m_\ell = -1$ minus the electron recoil term corresponding to $\mathbf{S}_\perp$ is

$$\Delta f = \frac{\Delta\omega}{2\pi} = \frac{E_{h\upsilon}}{h} = \frac{\left(E_{h\upsilon}\right)^2}{2hm_H c^2} = \frac{\left(13.5983\ eV\left(1-\frac{1}{2^2}\right)\left(1+\left(1-\sqrt{\frac{3}{4}}\right)\right)\right)^2}{2hm_H c^2} = 17.2249\ MHz \tag{122}$$

Momentum of the electron, atom, and photon are conserved. The total recoil energy is the sum of the electron component (Eq. (121)) and the atom component (Eq. (122)). Thus, the calculated recoil frequency, Δf_R, shift due to both components of momentum transfer is

$$\Delta f_R = 25.1883\ MHz + 17.2249\ MHz = 42.4132\ MHz \tag{123}$$

corresponding to an energy, E_R, of

$$E_R = 1.75407\ X\ 10^{-7}\ eV \tag{124}$$

The energy, E_{FS} and frequency, Δf_{FS}, for the $^2P_{3/2} \rightarrow {}^2P_{1/2}$ transition called the fine structure splitting is given by the sum of Eqs. (118), (121), and (122) and Eqs. (119) and (123), respectively:

$$\begin{aligned} E_{FS} &= \frac{\alpha^5(2\pi)^2}{8} m_e c^2 \sqrt{\frac{3}{4}} + \left(13.5983\ eV\left(1-\frac{1}{2^2}\right)\right)^2 \left[\frac{\left(\frac{3}{4\pi}\left(1-\sqrt{\frac{3}{4}}\right)\right)^2}{2h\mu_e c^2} + \frac{\left(1+\left(1-\sqrt{\frac{3}{4}}\right)\right)^2}{2hm_H c^2}\right] \\ &= 4.5190\ X\ 10^{-5}\ eV + 1.75407\ X\ 10^{-7}\ eV \\ &= 4.53659\ X\ 10^{-5}\ eV \end{aligned} \tag{125}$$

$$\Delta f_{FS} = 10,927.0\ MHz + 42.4132\ MHz = 10,969.4\ MHz \tag{126}$$

The energy of $4.53659\ X\ 10^{-5}\ eV$ corresponds to a frequency of $10,969.4\ MHz$ given by Eqs. (125) and (126), respectively, or a wavelength of $2.73298\ cm$. The experimental value of the

$^2P_{3/2}$—$^2P_{1/2}$ transition frequency is $10{,}969.1\ MHz$ [61, 63]. The large natural widths of the hydrogen $2p$ levels limits the experimental accuracy [63]; yet, given this limitation, the agreement between the theoretical and experimental fine structure is excellent and within the cited errors.

M. Spin-Nuclear Coupling (Hyperfine Structure)

The radius of the hydrogen atom is increased or decreased very slightly due to the Lorentzian force on the electron due to the magnetic field of the proton and its orientation relative to the electron's angular momentum vector. The additional small centripetal magnetic force is the relativistic corrected Lorentzian force, $\mathbf{F}_{mag}$, as also given in the Two-Electron Atom section and the Three, Four, Five, Six, Seven, Eight, Nine, Ten, Eleven, Twelve, Thirteen, Fourteen, Fifteen, Sixteen, Seventeen, Eighteen, Nineteen, and Twenty-Electron Atoms section of Ref. [7].

The orbitsphere with $\ell = 0$ is a shell of negative charge current comprising correlated charge motion along great circles. The superposition of the vector projection of the orbitsphere angular momentum on the z-axis is $\mathbf{L}_z = \frac{\hbar}{2}$ (Eq. (1.73b) of Ref. [7]) with an orthogonal component of $\mathbf{L}_{xy} = \frac{\hbar}{4}$ (Eq. (1.73a) of Ref. [7]). The magnetic field of the electron at the nucleus due to $\mathbf{L}_z$ after McQuarrie [45] is

$$\mathbf{B} = \frac{\mu_o e \hbar}{2 m_e r^3} \tag{127}$$

where μ_0 is the permeability of free-space ($4\pi X\, 10^{-7}\ N/A^2$). An electrodynamic force or radiation reaction force, a force dependent on the second derivative of the charge's position with

respect to time, arises between the electron and the proton. This force given in Sections 6.6, 12.10, and 17.3 of Jackson [64] achieves the condition that the sum of the mechanical momentum and electromagnetic momentum is conserved.

The magnetic moment of the proton, μ_P, aligns in the direction of $\mathbf{L}_z$, but experiences a torque due to the orthogonal component $\mathbf{L}_{xy}$. As shown in the Orbitsphere Equation of Motion for $\ell = 0$ section of Ref. [7], the magnetic field of the orbitsphere gives rise to the precession of the magnetic moment vector of the proton directed from the origin of the orbitsphere at an angle of $\theta = \frac{\pi}{3}$ relative to the z-axis. The precession of μ_P forms a cone in the nonrotating laboratory frame to give a perpendicular projection of

$$\mu_{P\perp} = \pm\sqrt{\frac{3}{4}}\mu_P \tag{128}$$

after Eq. (1.74a) of Ref. [7] and a projection onto the z-axis of

$$\mu_{P\parallel} = \pm\frac{\mu_P}{2} \tag{129}$$

after Eq. (1.74b) of Ref. [7]. At torque balance, $\mathbf{L}_{xy}$ also precesses about the z-axis at 90° with respect to $\mu_{P\parallel}$. Using Eq. (127), the magnitude of the force F_{mag} between the antiparallel field of the electron and μ_P is

$$F_{mag} = \left|\frac{\mu_P \times \mathbf{B}}{r}\right| = \mu_P \frac{\mu_o e\hbar}{2m_e r^4} \tag{130}$$

The radiation reaction force corresponding to photon emission or absorption is radial as given in the Equation of the Electric Field inside the Orbitsphere section of Ref. [7]. The reaction force on the electron due to the force of the electron's field on the magnetic moment of the proton is the corresponding relativistic central force, $\mathbf{F}_{mag}$, which acts uniformly on each charge (mass)-

density element of the electron. The magnetic central force is derived as follows from the Lorentzian force which is relativistically corrected. The Lorentzian force at each point of the electron moving at velocity **v** due to a magnetic flux **B** is

$$\mathbf{F}_{mag} = e\mathbf{v} \times \mathbf{B} \tag{131}$$

Eqs. (130) and (131) may be expressed in terms of the electron velocity given by Eq. (6):

$$F_{mag} = \frac{\hbar}{m_e r}\frac{e\mu_o \mu_P}{2r^3} = \frac{e}{2}|\mathbf{v} \times \mathbf{B}| \tag{132}$$

where **B** is the magnetic flux of the proton at the electron. (The magnetic moment **m** of the proton is $\mathbf{m} = \mu_P \mathbf{i}_z$, and the magnetic field of the proton follows from the relationship between the magnetic dipole field and the magnetic moment **m** as given by Jackson [65].) In the light-like frame, the velocity **v** is the speed of light, and **B** corresponds to the time dependent component of the proton magnetic moment given by Eq. (128). Thus, the central force is

$$\mathbf{F}_{mag} = \pm\frac{e\alpha c}{2}\frac{\mu_0}{r^3}\ \mu_P\sqrt{\frac{3}{4}} \tag{133}$$

where the relativistic factor from Eq. (1.217) of Ref. [7] is α and the plus corresponds to antiparallel alignment of the magnetic moments of the electron and proton, and the minus corresponds to parallel alignment. From Eq. (59), the outward centrifugal force (Eq. (1.209) of Ref. [7]) on the electron is balanced by the electric force (Eq. (1.210) of Ref. [7]) and the magnetic forces given by Eq. (1.221) of Ref. [7] and Eq. (133):

$$\frac{m_e v^2}{r} = \frac{e^2}{4\pi\varepsilon_o r^2} - \frac{\hbar^2}{mr^3} \pm \sqrt{\frac{3}{4}}\frac{e\alpha c}{2}\frac{\mu_0}{r^3}\ \mu_P \tag{134}$$

Using Eq. (6),

$$\frac{\hbar^2}{m_e r^3} = \frac{e^2}{4\pi\varepsilon_o r^2} - \frac{\hbar^2}{mr^3} \pm \sqrt{\frac{3}{4}}\frac{e\alpha c}{2}\frac{\mu_0}{r^3}\ \mu_P \tag{135}$$

$$\frac{\hbar^2}{m_e r^3} + \frac{\hbar^2}{m r^3} = \frac{e^2}{4\pi\varepsilon_o r^2} \pm \sqrt{\frac{3}{4}} \frac{e\alpha c}{2} \frac{\mu_0}{r^3} \mu_P \tag{136}$$

$$\frac{\hbar^2}{\mu_e} \pm \sqrt{\frac{3}{4}} \frac{e\alpha c \mu_0 \mu_P}{2} = \frac{e^2}{4\pi\varepsilon_o} r \tag{137}$$

$$r = a_H \pm \sqrt{\frac{3}{4}} \frac{4\pi\varepsilon_o}{2e^2} e \alpha c \mu_0 \mu_P \tag{138}$$

$$r = a_H \pm \sqrt{\frac{3}{4}} \frac{2\pi\alpha \mu_P}{ec} \tag{139}$$

where μ_e is the electron reduced mass given by Eq. (1.224) of Ref. [7], a_H is the radius of the hydrogen atom given by Eq. (1.228) of Ref. [7], the plus corresponds to parallel alignment of the magnetic moments of the electron and proton, and the minus corresponds to antiparallel alignment.

a. Energy Calculations

The magnetic energy to flip the orientation of the proton's magnetic moment, μ_P, from antiparallel to parallel to the direction of the magnetic flux $\mathbf{B}_s$ of the electron (180° rotation of the magnet moment vector) given by the first term of Eq. (36), and Eqs. (127), and (128) is

$$\begin{aligned} \Delta E_{mag}^{\text{proton spin}} &= -\frac{\mu_0 e\hbar}{2m_e} \mu_P \sqrt{\frac{3}{4}} \left(\frac{1}{r_+^3} + \frac{1}{r_-^3} \right) \\ &= -\mu_0 \mu_B \mu_P \sqrt{\frac{3}{4}} \left(\frac{1}{r_+^3} + \frac{1}{r_-^3} \right) \\ &= -1.918365\ X\ 10^{-24}\ J \end{aligned} \tag{140}$$

where the Bohr magneton, μ_B, is given by Eq. (26).

The change in the electric energy of the electron due to the slight shift of the radius of the electron is given by the difference between the electric energies associated with the two possible

orientations of the magnetic moment of the electron with respect to the magnetic moment of the proton, parallel versus antiparallel. Each electric energy is given by the substitution of the corresponding radius given by Eq. (139) into Eq. (64). The change in electric energy for the flip from antiparallel to parallel alignment, $\Delta E_{ele}^{S/N}$, is

$$\Delta E_{ele}^{S/N} = \frac{-e^2}{8\pi\varepsilon_o}\left[\frac{1}{r_+} - \frac{1}{r_-}\right] = 9.597048\ X\ 10^{-25}\ J \tag{141}$$

In addition, the interaction of the magnetic moments of the electron and proton increases the magnetic energy, E_{mag}, of the electron given by Eq. (30). The term of E_{mag} for the hyperfine structure of the hydrogen atom is similar to that of muonium given by Eq. (161) in Sec. IIIN:

$$\begin{aligned} E_{mag} &= -\left(1 + \left(\frac{2}{3}\right)^2 + \alpha\left(\cos\frac{\pi}{3}\right)^2\right)\frac{\pi\mu_o e^2\hbar^2}{m_e^{\ 2}}\left(\frac{1}{r_+^3} - \frac{1}{r_-^3}\right) \\ &= -\left(1 + \left(\frac{2}{3}\right)^2 + \frac{\alpha}{4}\right)4\pi\mu_o\mu_B^2\left(\frac{1}{r_+^3} - \frac{1}{r_-^3}\right) \\ &= 1.748861\ X\ 10^{-26}\ J \end{aligned} \tag{142}$$

where the contribution corresponding to electron spin gives the first term, 1, and the second term, $\left(\frac{2}{3}\right)^2$, corresponds to the rotation of the electron about the z-axis corresponding to the precession of $\mathbf{L}_{xy}$. The geometrical factor of $\frac{2}{3}$ for the rotation is given in the Derivation of the Magnetic Field section in Chapter One (Eq. (1.108)) and by Eq. (12.342), of Ref. [7] and the energy is proportional to the magnetic field strength squared according to Eq. (29). The relativistic factor from Eq. (1.217) and Eqs. (1.129) and (2.102) of Ref. [7] is α times $\left(\cos\frac{\pi}{3}\right)^2$ where the latter term is due to the nuclear magnetic moment oriented $\theta = \frac{\pi}{3}$ relative to the z-axis. The energy is proportional to the magnetic field strength squared according to Eq. (29).

The total energy of the transition from antiparallel to parallel alignment, $\Delta E_{total}^{S/N}$, is given as the sum of Eqs. (140-142):

$$\begin{aligned}\Delta E_{total}^{S/N} &= \Delta E_{mag}^{\text{proton spin}} + \Delta E_{ele}^{S/N} + E_{mag} \\ &= -1.918365\ X\ 10^{-24}\ J + 9.597048\ X\ 10^{-25}\ J + 1.748861\ X\ 10^{-26}\ J \\ &= -9.411714\ X\ 10^{-25}\ J\end{aligned} \tag{143}$$

The energy is expressed in terms of wavelength using the Planck relationship, Eq. (87):

$$\lambda = \frac{hc}{\Delta E_{total}^{S/N}} = 21.10610\ cm \tag{144}$$

The experimental value from the hydrogen maser is $21.10611\ cm$ [66]. The 21 cm line is important in astronomy for the determination of the presence of hydrogen. There is remarkable agreement between the calculated and experimental values of the hyperfine structure that is only limited by the accuracy of the fundamental constants in Eqs. (139-142).

N. Muonium Hyperfine Structure Interval

Muonium (μ^+e^-, M) is the hydrogenlike bound state of a positive muon and an electron. The solution of the ground state ($1^2S_{1/2}$) hyperfine structure interval of muonium, $\Delta\nu_{Mu}$, is similar to that of the hydrogen atom. The electron binds to the muon as both form concentric orbitspheres with a minimization of energy. From Eqs. (59) and (134), the outward centrifugal force (Eq. (1.209) of Ref. [7]) on the electron is balanced by the electric force (Eq. (1.210) of Ref. [7]) and the magnetic forces due to the inner positive muon given by Eq. (1.221) of Ref. [7] and Eq. (133). The resulting force balance equation is the same as that for the hydrogen atom given by Eq. (134) with the muon mass, m_μ, replacing the proton mass, m, and the muon magnetic moment, μ_μ, replacing the proton magnetic moment, μ_P. The radius of the electron, r_2, is given by

$$\frac{m_e v^2}{r_2} = \frac{e^2}{4\pi\varepsilon_o r_2^2} - \frac{\hbar^2}{m_\mu r_2^3} \pm \sqrt{\frac{3}{4}} \frac{e\alpha c}{2} \frac{\mu_0}{r_2^3} \mu_\mu \tag{145}$$

Using Eq. (6),

$$\frac{\hbar^2}{m_e r_2^3} = \frac{e^2}{4\pi\varepsilon_o r_2^2} - \frac{\hbar^2}{m_\mu r_2^3} \pm \sqrt{\frac{3}{4}} \frac{e\alpha c}{2} \frac{\mu_0}{r_2^3} \mu_\mu \tag{146}$$

$$\frac{\hbar^2}{\mu_{e,\mu}} \pm \sqrt{\frac{3}{4}} \frac{e\alpha c \mu_0 \mu_\mu}{2} = \frac{e^2}{4\pi\varepsilon_o} r_2 \tag{147}$$

$$r_2 = a_\mu \pm \sqrt{\frac{3}{4}} \frac{2\pi\alpha \mu_\mu}{ec} \tag{148}$$

$$r_{2+} = a_\mu + \sqrt{\frac{3}{4}} \frac{2\pi\alpha \mu_\mu}{ec} = 5.31736859 \, X \, 10^{-11} \, m \tag{149}$$

$$r_{2-} = a_\mu - \sqrt{\frac{3}{4}} \frac{2\pi\alpha \mu_\mu}{ec} = 5.31736116 \, X \, 10^{-11} \, m \tag{150}$$

where $\mu_{e,\mu}$ is the muonium electron reduced mass given by Eq. (1.224) of Ref. [7] with the mass of the proton replaced by the mass of the muon and a_μ is the Bohr radius of the muonium atom given by Eq. (170) with the electron reduced mass, μ_e (Eq. (1.224) of Ref. [7]), replaced by $\mu_{e,\mu}$. The plus sign corresponds to parallel alignment of the magnetic moments of the electron and muon, and the minus sign corresponds to antiparallel alignment.

The radii of the muon, r_1, in different spin states can be determined from r_2, the radii of the electron (Eqs. (149-150)), and the opposing forces on the muon due to the bound electron. The outward centrifugal force (Eq. (1.209) of Ref. [7]) on the muon is balanced by the reaction forces given by Eq. (145):

$$\frac{m_\mu v^2}{r_1} = \frac{\hbar^2}{m_e r_2^3} \pm \sqrt{\frac{3}{4}} \frac{e\alpha c}{2} \frac{\mu_0}{r_2^3} \mu_\mu \tag{151}$$

Using Eq. (6),

$$\frac{\hbar^2}{m_\mu r_1^3} = \frac{\hbar^2}{m_e r_2^3} \pm \sqrt{\frac{3}{4}} \frac{e\alpha c}{2} \frac{\mu_0}{r_2^3} \mu_\mu \tag{152}$$

$$r_2^3 = \left(\frac{m_\mu}{m_e} \pm \sqrt{\frac{3}{4}} \frac{m_\mu e \alpha c}{2\hbar^2} \mu_0 \mu_\mu \right) r_1^3 \tag{153}$$

$$r_1 = \frac{r_2}{\left(\frac{m_\mu}{m_e} \pm \sqrt{\frac{3}{4}} \frac{m_\mu e \alpha c}{2\hbar^2} \mu_0 \mu_\mu \right)^{1/3}} \tag{154}$$

Using Eqs. (149-150) for r_2,

$$r_1 = \frac{a_\mu \pm \sqrt{\frac{3}{4}} \frac{2\pi\alpha \mu_\mu}{ec}}{\left(\frac{m_\mu}{m_e} \pm \sqrt{\frac{3}{4}} \frac{m_\mu e \alpha c}{2\hbar^2} \mu_0 \mu_\mu \right)^{1/3}} \tag{155}$$

$$r_{1+} = \frac{a_\mu + \sqrt{\frac{3}{4}} \frac{2\pi\alpha \mu_\mu}{ec}}{\left(\frac{m_\mu}{m_e} + \sqrt{\frac{3}{4}} \frac{m_\mu e \alpha c}{2\hbar^2} \mu_0 \mu_\mu \right)^{1/3}} = 8.9922565 \ X \ 10^{-12} \ m \tag{156}$$

$$r_{1-} = \frac{a_\mu - \sqrt{\frac{3}{4}} \frac{2\pi\alpha \mu_\mu}{ec}}{\left(\frac{m_\mu}{m_e} - \sqrt{\frac{3}{4}} \frac{m_\mu e \alpha c}{2\hbar^2} \mu_0 \mu_\mu \right)^{1/3}} = 8.99224822 \ X \ 10^{-12} \ m \tag{157}$$

where the plus corresponds to parallel alignment of the magnetic moments of the electron and muon, and the minus corresponds to antiparallel alignment.

a. Energy Calculations

The magnetic energy, $\Delta E_{mag}^{spin}(\Delta\nu_{Mu})$, to flip the orientation of the muon's magnetic moment, μ_μ, from antiparallel to parallel to the direction of the magnetic flux $\mathbf{B}_s$ of the electron (180° rotation of the magnet moment vector) given by Eq. (140) is

$$\Delta E_{mag}^{spin}(\Delta\nu_{Mu}) = -\sqrt{\frac{3}{4}}\frac{\mu_0 e\hbar}{2m_e}\mu_\mu\left(\frac{1}{r_{2+}^3}+\frac{1}{r_{2-}^3}\right)$$
$$= -\sqrt{\frac{3}{4}}\mu_0\mu_B\mu_\mu\left(\frac{1}{r_{2+}^3}+\frac{1}{r_{2-}^3}\right) \quad (158)$$
$$= -6.02890320\ X\ 10^{-24}\ J$$

wherein the muon magnetic moment replaces the proton magnetic moment and the electron Bohr magneton, μ_B, is given by Eq. (26).

An electric field equivalent to that of a point charge of magnitude $+e$ at the origin only exists for $r_1 < r \le r_2$. Thus, the change in the electric energy of the electron due to the slight shift of the radius of the electron is given by the difference between the electric energies associated with the two possible orientations of the magnetic moment of the electron with respect to the magnetic moment of the muon, parallel versus antiparallel. Each electric energy is given by the substitution of the corresponding radius given by Eq. (148) into Eq. (64) or Eq. (141). The change in electric energy for the flip from antiparallel to parallel alignment, $\Delta E_{ele}(\Delta\nu_{Mu})$, is

$$\Delta E_{ele}(\Delta\nu_{Mu}) = \frac{-e^2}{8\pi\varepsilon_o}\left[\frac{1}{r_{2+}}-\frac{1}{r_{2-}}\right] = 3.02903048\ X\ 10^{-24}\ J \quad (159)$$

For each lepton, the application of a magnetic field with a resonant Larmor excitation gives rise to a precessing angular momentum vector **S** of magnitude $\hbar$ directed from the origin of the orbitsphere at an angle of $\theta = \frac{\pi}{3}$ relative to the applied magnetic field. As given in the Spin Angular Momentum of the Orbitsphere with $\ell = 0$ section of Ref. [7], **S** rotates about the axis of the applied field at the Larmor frequency. The magnitude of the components of **S** that are parallel and orthogonal to the applied field (Eqs (1.74a-1.74b) of Ref. [7]) are $\frac{\hbar}{2}$ and $\sqrt{\frac{3}{4}}\hbar$, respectively. Since both the RF field and the orthogonal components shown in Figure 1.7 of Ref.

[7] rotate at the Larmor frequency, the RF field that causes a Stern Gerlach transition produces a stationary magnetic field with respect to these components as described by Patz [67]. The corresponding central field at the orbitsphere surface given by the superposition of the central field of the lepton and that of the photon follows from Eqs. (2.10-2.17) and Eq. (17) of Box 1.2 of Ref. [7]:

$$\mathbf{E} = \frac{e}{4\pi\varepsilon_o r^2}\left[Y_0^0(\theta,\phi)\mathbf{i}_\mathbf{r} + \mathrm{Re}\left\{Y_\ell^m(\theta,\phi)e^{i\omega_n t}\right\}\mathbf{i}_\mathbf{y}\delta(r-r_1)\right] \tag{160}$$

where the spherical harmonic dipole $Y_\ell^m(\theta,\phi) = \sin\theta$ is with respect to the $\mathbf{S}$-axis. The dipole spins about the $\mathbf{S}$-axis at the angular velocity given by Eq. (9). The resulting current is nonradiative as shown Sec. IIID. Thus, the field in the RF rotating frame is magnetostatic as shown in Figure 1.9 of Ref. [7] but directed along the $\mathbf{S}$-axis.

The interaction of the magnetic moments of the leptons increases their magnetic energies given by Eq. (30) with the mass of the corresponding lepton:

$$\begin{aligned} E_{mag,e}^{stored}(\Delta\nu_{Mu}) &= -\left(1+\left(\frac{2}{3}\cos\frac{\pi}{3}\right)^2+\alpha\right)\frac{\pi\mu_o e^2\hbar^2}{m_e^{\ 2}}\left(\frac{1}{r_{2+}^3}-\frac{1}{r_{2-}^3}\right) \\ &= -\left(1+\left(\frac{2}{3}\cos\frac{\pi}{3}\right)^2+\alpha\right)4\pi\mu_o\mu_B^2\left(\frac{1}{r_{2+}^3}-\frac{1}{r_{2-}^3}\right) \\ &= 4.23209178\ X\ 10^{-26}\ J \end{aligned} \tag{161}$$

$$\begin{aligned} E_{mag,\mu}^{stored}(\Delta\nu_{Mu}) &= -\left(1+\left(\frac{2}{3}\cos\frac{\pi}{3}\right)^2+\alpha\right)\frac{\pi\mu_o e^2\hbar^2}{m_\mu^{\ 2}}\left(\frac{1}{r_{1+}^3}-\frac{1}{r_{1-}^3}\right) \\ &= -\left(1+\left(\frac{2}{3}\cos\frac{\pi}{3}\right)^2+\alpha\right)4\pi\mu_o\mu_{B,\mu}^2\left(\frac{1}{r_{1+}^3}-\frac{1}{r_{1-}^3}\right) \\ &= 1.36122030\ X\ 10^{-28}\ J \end{aligned} \tag{162}$$

where 1.) the radii of the electron and muon are given by Eq. (149-150) and Eqs. (156-157)), respectively, 2.) $\mu_{B,\mu}$ is the muon Bohr magneton given by Eq. (26) with the electron mass replaced by the muon mass, 3.) the first term is due to lepton spin, 4.) the second term,

$\left(\frac{2}{3}\cos\frac{\pi}{3}\right)^2$ is due to **S**, oriented $\theta = \frac{\pi}{3}$ relative to the z-axis, wherein the geometrical factor of $\frac{2}{3}$ corresponds to the source current of the dipole field (Eq. (160)) given in the Derivation of the Magnetic Field section in Chapter One (Eq. (1.108)) and by Eq. (12.342) of Ref. [7], and the energy is proportional to the magnetic field strength squared according to Eq. (29), and 5.) the relativistic factor from Eq. (1.217) and Eqs. (1.129) and (2.102) of Ref. [7] is α.

The energy of the ground state ($1^2S_{1/2}$) hyperfine structure interval of muonium, $\Delta E(\Delta\nu_{Mu})$, is given by the sum of Eqs. (158-159) and (161-162):

$$\begin{aligned}\Delta E(\Delta\nu_{Mu}) &= \Delta E^{spin}_{mag}(\Delta\nu_{Mu}) + \Delta E_{ele}(\Delta\nu_{Mu}) + E^{stored}_{mag,e}(\Delta\nu_{Mu}) + E^{stored}_{mag,\mu}(\Delta\nu_{Mu}) \\ &= -6.02890320\ X\ 10^{-24}\ J + 3.02903048\ X\ 10^{-24}\ J + 4.23209178\ X\ 10^{-26}\ J + 1.36122030\ X\ 10^{-28}\ J \\ &= -2.95741568\ X\ 10^{-24}\ J\end{aligned} \tag{163}$$

Using Planck's equation (Eq. (87)), the interval frequency, $\Delta\nu_{Mu}$, and wavelength, $\Delta\lambda_{Mu}$, are

$$\Delta\nu_{Mu} = 4.46330328\ GHz \tag{164}$$

$$\Delta\lambda_{Mu} = 6.71682919\ \text{cm} \tag{165}$$

The experimental hyperfine structure interval of muonium [68] is

$$\begin{aligned}&\Delta E(\Delta\nu_{Mu}) = -2.957415336\ X\ 10^{-24}\ J \\ &\Delta\nu_{Mu} = 4.463302765(53)\ GHz\ (12\ ppm) \\ &\Delta\lambda_{Mu} = 6.71682998\ \text{cm}\end{aligned} \tag{166}$$

There is remarkable (7 to 8 significant figure) agreement between the calculated and experimental values of $\Delta\nu_{Mu}$ that is only limited by the accuracy of the fundamental constants in Eqs. (156-159) and (161-162) as shown by using different CODATA values [46, 69-70].

O. Positronium

Pair production, the creation of a positron/electron pair, occurs such that the radius of one orbitsphere has a radius infinitesimally greater than the radius of the antiparticle orbitsphere as discussed in the Pair Production section and the Leptons section of Ref. [7]. In addition, a minimum energy may be obtained by the binding of a positron and an electron as concentric orbitspheres at the same radius such that the electric fields mutually cancel with the conservation of $\hbar$ of angular momentum of each lepton. The short-lived hydrogen-like atom comprising an electron and a positron is called positronium. Before annihilation, positronium can exist with the electron and positron spins parallel or antiparallel called orthopositronium ($^3S_1$) and parapositronium ($^1S_0$), respectively. Due to the opposite charge of the positron, the magnetic moments are opposed to the spin orientations. The respective decay times are 1 ns and 1 μs. The splitting of the spectral lines due to spin orientations is called the hyperfine structure of positronium.

The forces of positronium are central, and the radius of the outer orbitsphere (electron or positron) is calculated as follows after Eqs. (59) (134), and (145). The centrifugal force is given by Eq. (1.209) of Ref. [7]. The centripetal electric force of the inner orbitsphere on the outer orbitsphere is given by Eq. (1.210) of Ref. [7]. A second centripetal force is the relativistic corrected magnetic force, $\mathbf{F}_{mag}$, between each point of the particle and the antiparticle given by Eq. (1.221) of Ref. [7] with m_e substituted for m. The force balance equation is given by Eq. (1.222) of Ref. [7] with m_e substituted for m. The balance between the centrifugal and electric and magnetic forces is given in the Excited States of the One-Electron Atom (Quantization) section and the Excited States of Helium section of Ref. [7] and Ref. [6]:

$$\frac{m_e v^2}{r_1} = \frac{\hbar^2}{m_e r_1^3} = \frac{e^2}{4\pi\varepsilon_o r_1^2} - \frac{\hbar^2}{m_e r_1^3} \tag{167}$$

$$r_1 = \frac{4\pi\varepsilon_0\hbar^2}{e^2\mu} \tag{168}$$

where $r_1 = r_2$ is the radius of the positron and the electron and where the reduced mass , μ , is

$$\mu = \frac{m_e}{2} \tag{169}$$

The Bohr radius given by

$$a_0 = \frac{4\pi\varepsilon_0\hbar^2}{e^2 m_e} \tag{170}$$

and Eq. (169) is substituted into Eq. (168) to give the ground-state radius of positronium:

$$r_1 = 2a_0 \tag{171}$$

a. Excited State Energies

The potential energy V between the particle and the antiparticle having the radius r_1 given by Eq. (61) is

$$V = \frac{-e^2}{4\pi\varepsilon_0 r_1} = \frac{-Z^2e^2}{8\pi\varepsilon_0 a_0} = -2.18375\ X\ 10^{-18}\ J = 13.59\ eV \tag{172}$$

The calculated ionization energy is $\frac{1}{2}V$ (Eqs. (62-64)) which is

$$E_{ele} = 6.795\ eV \tag{173}$$

The experimental ionization energy is $6.795\ eV$.

Parapositronium, a singlet state hydrogen-like atom comprising an electron and a positron, can absorb a photon which excites the atom to the first triplet state, orthopositronium. In parapositronium, the electron and positron angular momentum vectors are antiparallel; whereas, the magnetic moment vectors are parallel. The opposite relationships exist for orthopositronium. The balance between the centrifugal and electric and magnetic forces is

$$\frac{m_e v^2}{r_n} = \frac{\hbar^2}{m_e r_n^3} = \frac{1}{n}\frac{e^2}{4\pi\varepsilon_0 r_n^2} - \frac{\hbar^2}{m_e r_n^3} \tag{174}$$

$$r_n = n2a_0 \tag{175}$$

where n is an integer and both electrons are at the same excited state radius of $r_n = n2a_o$. The principal energy levels for the singlet excited states are given by Eq. (2.22) and Eq. (9.12) of Ref. [7] with the electron reduced mass (Eq. (169)) substituted for the mass of the electron.

$$E_n = \frac{1}{n}\frac{e^2\mu}{8\pi\varepsilon_0 r_n} = \frac{1}{n}\frac{e^2\mu}{8\pi\varepsilon_0 n a_0} = \frac{6.795}{n^2}\ eV \tag{176}$$

The levels given by Eq. (176) match the experimental energy levels.

b. Hyperfine Structure

As shown in the Spin Angular Momentum of the Orbitsphere with $\ell = 0$ section of Ref. [7], the angular momentum of the electron or positron orbitsphere in a magnetic field comprises the initial $\frac{\hbar}{2}$ projection on the z-axis and the initial $\frac{\hbar}{4}$ vector component in the xy-plane that precesses about the z-axis. As further shown in the Magnetic Parameters of the Electron (Bohr Magneton) section of Ref. [7], a resonant excitation of the Larmor precession frequency gives rise to an additional component of angular momentum which is consistent with Maxwell's equations. As shown in the Excited States of the One-Electron Atom (Quantization) section of Ref. [7], conservation of the $\hbar$ of angular momentum of a trapped photon can give rise to $\hbar$ of electron angular momentum along the **S**-axis. The photon standing waves of excited states are spherical harmonic functions which satisfy Laplace's equation in spherical coordinates and provide the force balance for the corresponding charge (mass)-density waves. Consider the photon in the case of the precessing electron with a Bohr magneton of magnetic moment along

the **S**-axis. The radius of the orbitsphere is unchanged, and the photon gives rise to current on the surface that satisfies the condition

$$\nabla \cdot J = 0 \tag{177}$$

corresponding to a rotating spherical harmonic dipole [7] that phase-matches the current (mass) density of Eq. (1.112) of Ref. [7]. Thus, the electrostatic energy is constant, and only the magnetic energy need be considered as given by Eqs. (179-180). The corresponding central field at the orbitsphere surface given by the superposition of the central field of the lepton and that of the photon follows from Eqs. (2.10-2.17) and Eq. (17) of Box 1.2 of Ref. [7] and is the spherical harmonic dipole with respect to the **S**-axis given by Eq. (160). The dipole spins about the **S**-axis at the angular velocity given by Eq.(9). The resulting current is nonradiative as shown in Sec. IIID. Thus, the field in the RF rotating frame is magnetostatic as shown in Figure 1.9 of Ref. [7] but directed along the **S**-axis.

The application of a magnetic field with a resonant Larmor excitation gives rise to a precessing angular momentum vector **S** of magnitude $\hbar$ directed from the origin of the orbitsphere at an angle of $\theta = \frac{\pi}{3}$ relative to the applied magnetic field. **S** rotates about the axis of the applied field at the Larmor frequency. The magnitude of the components of **S** that are parallel and orthogonal to the applied field (Eqs (1.74a-1.74b) of Ref. [7]) are $\frac{\hbar}{2}$ and $\sqrt{\frac{3}{4}}\hbar$, respectively. Since both the RF field and the orthogonal components shown in Figure 1.7 of Ref. [7] rotate at the Larmor frequency, the RF field that causes a Stern Gerlach transition produces a stationary magnetic field with respect to these components as described by Patz [67].

The component of Eq. (1.74b) of Ref. [7] adds to the initial $\frac{\hbar}{2}$ parallel component to give

a total of $\hbar$ in the stationary frame corresponding to a Bohr magneton, μ_B, of magnetic moment. The potential energy of a magnetic moment $\mathbf{m}$ in the presence of flux $\mathbf{B}$ [45] is

$$E = \mathbf{m} \cdot \mathbf{B} \tag{178}$$

The angular momentum of the electron gives rise to a magnetic moment of μ_B. Thus, the energy ΔE_{mag}^{spin} to switch from parallel to antiparallel to the field is given by Eq. (1.136) of Ref. [7]:

$$\Delta E_{mag}^{spin} = 2\mu_{\mathbf{B}}\,\mathbf{i_z} \cdot \mathbf{B} = 2\mu_B B\cos\theta = 2\mu_B B \tag{179}$$

ΔE_{mag}^{spin} is also given by Planck's equation. It can be shown from conservation of angular momentum considerations (Eqs. (26-34) of Box 1.2 of Ref. [7]) that the Zeeman splitting is given by Planck's equation and the Larmor frequency based on the gyromagnetic ratio (Eq. (2) of Box 1.2 of Ref. [7]). The electron's magnetic moment may only be parallel or antiparallel to the magnetic field rather than at a continuum of angles including perpendicular according to Eq. (178). No continuum of energies predicted by Eq. (178) for a pure magnetic dipole is possible. The energy difference for the magnetic moment to flip from parallel to antiparallel to the applied field is

$$\Delta E_{mag}^{spin} = 2\hbar\omega_L \tag{180}$$

corresponding to magnetic dipole radiation wherein ω_L is the Larmor angular frequency.

Eq. (178) implies a continuum of energies; whereas, Eq. (29) of Box 1.2 of Ref. [7] shows that the static-kinetic and dynamic vector potential components of the angular momentum are quantized at $\frac{\hbar}{2}$. Consequently, as shown in Sec. IIIG and the Electron g Factor section of Ref. [7], the flux linked during a spin transition is quantized as the magnetic flux quantum, $\Phi_0 = \frac{h}{2e}$. Only the states corresponding to $m_s = \pm\frac{1}{2}$ are possible due to conservation of angular

momentum. It is further shown using the Poynting power vector with the requirement that flux is linked in units of the magnetic flux quantum, that the factor 2 of Eqs. (179) and (180) is replaced by the electron g factor. The energy ΔE_{mag}^{spin} to flip the electron's magnetic moment from parallel to antiparallel to the applied field is given by Eqs. (36-37).

Positronium undergoes a Stern-Gerlach transition. The energy of the transition from orthopositronium ($^3S_1$) to parapositronium ($^1S_0$) is the hyperfine structure interval. The angular momentum of the photon given by $\mathbf{m} = \int \frac{1}{8\pi c} \mathrm{Re}[\mathbf{r} \times (\mathbf{E} \times \mathbf{B}^*)] dx^4 = \hbar$ in the Photon section of Ref. [7] is conserved [57] for the solutions for the resonant photons and hyperfine-state lepton functions as shown for the cases of one-electron atoms and helium in the Excited States of the One-Electron Atom (Quantization) section and the Excited States of Helium section of Ref. [7], respectively, and Ref. [6]. To conserve the $\hbar$ of angular momentum of each lepton and the photon, orthopositronium possesses orbital angular momentum states corresponding to $m_\ell = 0, \pm 1$; whereas, parapositronium possesses orbital angular momentum states corresponding to the quantum number $m_\ell = 0$. The orbital angular momentum states of orthopositronium are degenerate in the absence of an applied magnetic field. As in the case of the electron Stern-Gerlach transition, the radius of both leptons remains at the same radius of $r = 2a_0$ given by Eq. (171).

The hyperfine structure interval of positronium can be calculated from the spin-spin and spin-orbital coupling energies of the $^3S_1 \rightarrow {}^1S_0$ transition. The vector projection of the orbitsphere angular momentum on the z-axis is $\mathbf{L}_z = \frac{\hbar}{2}$ (Eq. (1.73b) of Ref. [7]) with an orthogonal component of $\mathbf{L}_{xy} = \frac{\hbar}{4}$ (Eq. (1.73a) of Ref. [7]). The magnetic flux, $\mathbf{B}$, of the electron (positron)

at the positron (electron) due to $\mathbf{L}_z$ after McQuarrie [45] is given by Eq. (127). The spin-spin coupling energy $\Delta E_{\text{spin-spin}}$ between the inner orbitsphere and the outer orbitsphere is given by Eq. (37) where μ_B, the magnetic moment of the outer orbitsphere is given by Eq. (26). Substitution of Eqs. (26) and (127) into Eq. (37) gives

$$\begin{aligned}\Delta E_{\text{spin-spin}} &= \frac{1}{2}\frac{g\mu_o e^2\hbar^2}{4m_e^2 r_1^3} \\ &= \frac{g\mu_o e^2\hbar^2}{8m_e^2(2a_0)^3} \\ &= \frac{1}{8\pi\alpha}\frac{g\alpha^5(2\pi)^2}{8}m_e c^2\end{aligned} \tag{181}$$

where the factor of $1/2$ arises from Eq. (178) with the presence of the magnetic flux only for the ${}^1S_0$ state, the radius is given by Eq. (171), and Eqs. (115-118) were used to convert Eq. (181) to the electron mass-energy form of Eq. (118).

In the case of atomic hydrogen with $n = 2$, the radius given by Eq. (2.2) of Ref. [7] is $r = 2a_0$, and the predicted energy difference between the ${}^2P_{3/2}$ and ${}^2P_{1/2}$ levels of the hydrogen atom, $E_{s/o}$, is given by Eq. (118). In the case of the hyperfine transition of positronium, the spin-orbital coupling energy $\Delta E_{s/o}({}^3S_1 \rightarrow {}^1S_0)$ having $r = 2a_0$ is given by Eq. (118) with the requirement that the flux from the partner lepton is linked in units of the magnetic flux quantum corresponding to the anomalous g factor (Eqs. (36-37)), the source current given by Eq. (160) gives rise to a factor of $3/2$, and each lepton contributes to the energy:

$$\Delta E_{s/o}({}^3S_1 \rightarrow {}^1S_0) = 2\frac{3}{2}\frac{g\alpha^5(2\pi)^2}{8}m_e c^2\sqrt{\frac{3}{4}} \tag{182}$$

The hyperfine structure interval of positronium (${}^3S_1 \rightarrow {}^1S_0$) is given by the sum of Eqs. (181) and (182):

$$\begin{aligned}\Delta E_{\text{Ps hyperfine}} &= \Delta E_{\text{spin -spin}} + \Delta E_{s/o}({}^3S_1 \rightarrow {}^1S_0) \\ &= \frac{g\mu_o e^2\hbar^2}{8m_e^2(2a_0)^3} + \frac{3g\alpha^5(2\pi)^2}{8} m_e c^2 \sqrt{\frac{3}{4}} \\ &= \frac{g\alpha^5(2\pi)^2}{8} m_e c^2 \left(\frac{1}{8\pi\alpha} + \frac{3\sqrt{3}}{2}\right) \\ &= 8.41155110\ X\ 10^{-4}\ eV\end{aligned} \tag{183}$$

Using Planck's equation (Eq. (87)), the interval in frequency, $\Delta\upsilon$, is

$$\Delta\upsilon = \ 203.39041\ GHz \tag{184}$$

The experimental ground-state hyperfine structure interval [71] is

$$\begin{aligned}&\Delta E_{\text{Ps hyperfine}}(\text{experimental}) = 8.41143\ X\ 10^{-4}\ eV \\ &\Delta\upsilon(\text{experimental}) = 203.38910(74)\ GHz\ (3.6\ ppm)\end{aligned} \tag{185}$$

There is remarkable (six significant figure) agreement between the calculated and experimental values of $\Delta\upsilon$ that is only limited by the accuracy of the fundamental constants [70]. A computer simulation of positronium and the positron-electron-annihilation event is shown in the Positronium section of Ref. [7].

IV. Conclusion

It is true that the Schrödinger equation can be solved exactly for the hydrogen atom; although, it is not true that the result is the exact solution of the hydrogen atom. Electron spin is missed entirely, and there are many internal inconsistencies and nonphysical consequences that do not agree with experimental results [1-10]. Despite its successes, quantum mechanics (QM) has remained mysterious to all who have encountered it. Starting with Bohr and progressing into the present, the departure from intuitive, physical reality has widened. The connection between quantum mechanics and reality is more than just a "philosophical" issue. It reveals that quantum mechanics is not a correct or complete theory of the physical world and that inescapable internal

inconsistencies and incongruities arise when attempts are made to treat it as a physical as opposed to a purely mathematical "tool". But, QM has severe limitations even as a tool considering that beyond one-electron atoms, multielectron-atom quantum mechanical equations can not be solved except by approximation methods [12] involving adjustable-parameter theories that often involve new physics or constructs or are simply curve fitting algorithms [6].

Even the Schrödinger equation results for one-electron atoms (the only problem that can be solved without approximations) are not accurate at all. It is nonrelativistic and there are major differences between predicted and experimental ionization energies as Z increases. Furthermore, in addition to spin, it misses the Lamb shift, anomalous magnetic moment of the electron, the fine structure, the hyperfine structure, and spectra of positronium and muonium, it is not stable to radiation, and has many other problems with predictions that do not match experimentation [2-10]. It also has an infinite number of solutions, not just the ones given in textbooks as given in Margenau and Murphy [11] and Ref. [9].

The Dirac equation is touted as remedying the nonrelativistic nature of the Schrödinger equation and providing an argument for the existence of virtual particles and corresponding so-called quantum electrodynamics (QED) computer algorithms for calculating unexpected observables such as the Lamb shift and the anomalous magnetic moment of the electron. But, both the Schrödinger and Dirac equations have many problems which make them untenable as representing reality as discussed *supra*.—infinities, lack of Einstein causality (spooky action at a distance), self interaction, instability to radiation, negative kinetic energy states, Klein paradox, and more [1-10]. This was argued by the founders of quantum mechanics [22, 30-31]. Furthermore, QED is completely postulated. It involves a point electron which can not occupy any volume; consequently, all calculations have "intrinsic infinities" and require renormalization

which is completely arbitrary. It further relies on a string of nonphysical constructs. For example, it is based on postulated polarization of the vacuum by postulated virtual particles which have no basis in reality, are fantastical at best, and conclusively shown to be impossible based on special relativity and astrophysical observations [21].

Rather than invoking renormalization, untestable virtual particles, and polarization of the vacuum by the virtual particles, the results of QED such as the anomalous magnetic moment of the electron, the Lamb Shift, the fine structure and hyperfine structure of the hydrogen atom, and the hyperfine structure intervals of positronium and muonium (thought to be only solvable using QED) are solved exactly from Maxwell's equations.

$(g-2)/2$ is solved in closed form based on conservation of the electron's angular momentum and the subsequent requirement that flux must be linked by the extended electron in quantized units of the magnetic flux quantum $\Phi_0 = \frac{h}{2e}$. The Lamb shift is calculated from the conservation of momentum of the emitted photon and the recoiling electron and hydrogen atom. The fine structure energy is the Lamb-shifted relativistic interaction energy between the spin and orbital magnetic moments due to the corresponding angular momenta. The hyperfine structure of the hydrogen atom and muonium are calculated from the force balance contribution between the electron and the proton and muon, respectively. The transition energies correspond to the Stern-Gerlach and stored electric and magnetic energy changes. With positronium, the leptons are at the same radius, and the positronium hyperfine interval is given by the sum of the Stern-Gerlach and fine structure energies. In each case, the agreement is to the limit possible based on experimental measurements and the error of the measured fundamental constants in the closed-form equations containing only these constants. These results from the known physical laws based on direct observation invalidate virtual particles and confirm QED's illegitimacy as

representative of reality.

The laws of electromagnetism and electrodynamics summarized in Maxwell's equations predate quantum mechanics by over 100 years. These laws and the implicit special relativity are the most experimentally proven physical laws ever. They hold over at least 24 orders of magnitude of length scale [72]. It is evident that only theories consistent with Maxwell's equations and special relativity need be considered. By discovering the means to extend these laws to problems thought only solvable using the mechanics of QED, it is shown that Maxwell's equations are fact and the virtual-particle based QED is fiction.

References

1. F. Laloë, Do we really understand quantum mechanics? Strange correlations, paradoxes, and theorems, Am. J. Phys. 69 (6), June 2001, 655-701.
2. R. L. Mills, "The Fallacy of Feynman's Argument on the Stability of the Hydrogen Atom According to Quantum Mechanics," submitted; posted at http://www.blacklightpower.com/theory/theorypapers/Fallacy_Feynmans_Argument_030705.pdf.
3. R. L. Mills, "Classical Quantum Mechanics", Physics Essays, 16, (2003), pp. 433-498.
4. R. L. Mills, "Exact Classical Quantum Mechanical Solutions for One- Through Twenty-Electron Atoms", submitted; posted at http://www.blacklightpower.com/theory/theorypapers/Exact_Solutions_1-20_Electron_Atoms_102804.pdf.
5. R. L. Mills, "The Nature of the Chemical Bond Revisited and an Alternative Maxwellian Approach", submitted; posted at http://www.blacklightpower.com/theory/theorypapers/NatureChemicalBondRevisited%20102805.pdf.
6. R. L. Mills, "Exact Classical Quantum Mechanical Solution for Atomic Helium Which

Predicts Conjugate Parameters from a Unique Solution for the First Time", submitted; posted at http://www.blacklightpower.com/theory/theorypapers/Exact_Solutions_Atomic_Helium_102804.pdf.

7. R. L. Mills, *The Grand Unified Theory of Classical Quantum Mechanics*, January 2006 Edition posted at http://www.blacklightpower.com/theory/book.shtml.

8. R. L. Mills, "The Grand Unified Theory of Classical Quantum Mechanics", Int. J. Hydrogen Energy, Vol. 27, No. 5, (2002), pp. 565-590.

9. R. L. Mills, "The Nature of Free Electrons in Superfluid Helium--a Test of Quantum Mechanics and a Basis to Review its Foundations and Make a Comparison to Classical Theory", Int. J. Hydrogen Energy, Vol. 26, No. 10, (2001), pp. 1059-1096.

10. R. L. Mills, "The Hydrogen Atom Revisited", Int. J. of Hydrogen Energy, Vol. 25, Issue 12, December, (2000), pp. 1171-1183.

11. H. Margenau, G. M. Murphy, The Mathematics of Chemistry and Physics, D. Van Nostrand Company, Inc., New York, (1943), pp. 77-78.

12. D. A. McQuarrie, *Quantum Chemistry*, University Science Books, Mill Valley, CA, (1983), p. 291.

13. H. Margenau, G. M. Murphy, *The Mathematics of Chemistry and Physics*, 2nd ed, Krieger Publishing: Huntington, NY, 1976.

14. H. J. Maris, Journal of Low Temperature Physics, Vol. 120, (2000), p. 173.

15. C. A. Fuchs and A. Peres, "Quantum Theory Needs No "Interpretation", Physics Today, Vol. 53, March (2000), p. 70.

16. S. Peil, G. Gabrielse, "Observing the Quantum Limit of an Electron Cyclotron: QND Measurements of Quantum Jumps between Fock States, Phys. Rev. Lett., Volume 83, No. 7,

August 16, (1999), pp. 1287-1290.

17. F. J. Dyson, "Feynman's proof of Maxwell equations", Am. J. Phys., Vol. 58, (1990), pp. 209-211.
18. J. Horgan, "Quantum Philosophy", Scientific American, Vol. 267(1), July, (1992), p. 94.
19. V. F. Weisskopf, Reviews of Modern Physics, Vol. 21, No. 2, (1949), pp. 305-315.
20. A. Beiser, *Concepts of Modern Physics*, Fourth Edition, McGraw-Hill Book Company, New York, (1978), pp. 119-122.
21. M. M. Waldrop, Science, Vol. 242, (1988), pp. 1248-1250.
22. A. Einstein, B. Podolsky, N. Rosen, Phys. Rev., Vol. 47, (1935), p. 777.
23. H. Wergeland, "The Klein Paradox Revisited", in *Old and New Questions in Physics, Cosmology, Philosophy, and Theoretical Biology*, A. van der Merwe, Editor, Plenum Press: New York, (1983), pp. 503-515.
24. W. E. Lamb, R. C. Retherford, "Fine Structure of the Hydrogen Atom by a Microwave Method", R. C., Phys. Rev., Vol. 72, No. 3, August 1, (1947), pp. 241-243.
25. H. A. Bethe, P. A. M. Dirac, W. Heisenberg, E. P. Wigner, *From a Life of Physics*, Ed. A. Salam, et al., World Scientific, Singapore, (1989).
26. P. W. Milonni, *The Quantum Vacuum: An Introduction to Quantum Electrodynamics*, Academic Press, Inc. Boston, (1994), p. 90.
27. P. A. M. Dirac, *Directions in Physics*, ed. H. Hora and J. R. Shepanski, Wiley, New York, (1978), p. 36.
28. H. Dehmelt, "Experiments on the structure of an individual elementary particle, Science, (1990), Vol. 247, pp. 539-545.
29. H. A. Bethe., The Electromagnetic Shift of Energy Levels", Physical Review, Vol. 72, No. 4,

August, 15, (1947), pp. 339-341.

30. L. de Broglie, "On the true ideas underlying wave mechanics", *Old and New Questions in Physics, Cosmology, Philosophy, and Theoretical Biology*, A. van der Merwe, Editor, Plenum Press, New York, (1983), pp. 83-86.
31. D. C. Cassidy, *Uncertainty: the Life and Science of Werner Heisenberg*, W. H. Freeman and Company, New York, (1992), pp. 224-225.
32. P. J. Mohr, B. N. Taylor, "CODATA recommended values of the fundamental physical constants: 1998", Reviews of Modern Physics, Vol. 72, No. 2, April, (2000), pp. 376-378; p. 474
33. P. W. Milonni, *The Quantum Vacuum An Introduction to Quantum Electrodynamics*, Academic Press, Inc. Boston, (1994), pp. 107-111.
34. P. W. Milonni, *The Quantum Vacuum An Introduction to Quantum Electrodynamics*, Academic Press, Inc. Boston, (1994), p. 108.
35. G. P. Lepage, "Theoretical advances in quantum electrodynamics, International Conference on Atomic Physics, Atomic Physics; Proceedings, Singapore, World Scientific, Vol. 7, (1981), pp. 297-311.
36. G. Landvogt, "The Grand Unified Theory of Classical Quantum Mechanics", International Journal of Hydrogen Energy, Vol. 28, No. 10, (2003), pp. 1155.
37. P. Pearle, Foundations of Physics, "Absence of radiationless motions of relativistically rigid classical electron", Vol. 7, Nos. 11/12, (1977), pp. 931-945.
38. F. Dyson, "Feynman's proof of Maxwell equations", Am. J. Phys., Vol. 58, (1990), pp. 209-211.
39. H. A. Haus, "On the radiation from point charges", American Journal of Physics, Vol. 54,

(1986), 1126–1129.

40. http://www.blacklightpower.com/new.shtml.
41. D. A. McQuarrie, *Quantum Chemistry*, University Science Books, Mill Valley, CA, (1983), pp. 206-225.
42. J. Daboul and J. H. D. Jensen, Z. Physik, Vol. 265, (1973), pp. 455-478.
43. T. A. Abbott and D. J. Griffiths, Am. J. Phys., Vol. 53, No. 12, (1985), pp. 1203-1211.
44. G. Goedecke, Phys. Rev 135B, (1964), p. 281.
45. D. A. McQuarrie, *Quantum Chemistry*, University Science Books, Mill Valley, CA, (1983), pp. 238-241.
46. R. C. Weast, *CRC Handbook of Chemistry and Physics*, 68 th Edition, CRC Press, Boca Raton, Florida, (1987-88), p. F-186 to p. F-187.
47. R. S. Van Dyck, Jr., P. Schwinberg, H. Dehmelt, "New high precision comparison of electron and positron g factors", Phys. Rev. Lett., Vol. 59, (1987), p. 26-29.
48. E. R. Williams, P. T. Olsen, Phys. Rev. Lett. Vol. 42, (1979), p. 1575.
49. K. v. Klitzing, G. Dorda, M. Pepper, "New method for high-accuracy determination of the fine-structure constant based on Hall resistance", Phys. Rev. Lett. Vol. 45, (1980), pp. 494-497.
50. C. E. Moore, "Ionization Potentials and Ionization Limits Derived from the Analyses of Optical Spectra, Nat. Stand. Ref. Data Ser.-Nat. Bur. Stand. (U.S.), No. 34, 1970.
51. R. C. Weast, *CRC Handbook of Chemistry and Physics*, 58 Edition, CRC Press, West Palm Beach, Florida, (1977), p. E-68.
52. J. D. Jackson, *Classical Electrodynamics*, Second Edition, John Wiley & Sons, New York, (1975), pp. 758-763.

53. W. McC. Siebert, *Circuits, Signals, and Systems*, The MIT Press, Cambridge, Massachusetts, (1986), pp. 488-502.

54. D. A. McQuarrie, *Quantum Chemistry*, University Science Books, Mill Valley, CA, (1983), pp. 135-140.

55. T. C. Gibb, *Principles of Mössbauer Spectroscopy*, Chapman and Hall: London (1977), Chp. 1.

56. U. Gonser, From a Strange Effect to Mössbauer Spectroscopy in *Mössbauer Spectroscopy*, U. Gonser, Ed. Springer-Verlag: New York (1975), pp. 1-51.

57. J. D. Jackson, *Classical Electrodynamics*, Second Edition, John Wiley & Sons, New York, (1975), pp. 739-779.

58. J. D. Jackson, *Classical Electrodynamics*, Second Edition, John Wiley & Sons, New York, (1975), pp. 236-240.

59. L. C. Shen, J. A. Kong, *Applied Electromagnetism*, Brooks/Cole Engineering Division, Monterey, CA, (1983), pp. 170-209.

60. D. A. McQuarrie, *Quantum Chemistry*, University Science Books, Mill Valley, CA, (1983), pp. 27-28.

61. P. J. Mohr, B. N. Taylor, "CODATA recommended values of the fundamental physical constants: 1998", Reviews of Modern Physics, Vol. 72, No. 2, April, (2000), p. 371.

62. J. D. Jackson, *Classical Electrodynamics*, Second Edition, John Wiley & Sons: New York, (1975), pp. 503-561.

63. P. J. Mohr, B. N. Taylor, "CODATA recommended values of the fundamental physical constants: 1998", Reviews of Modern Physics, Vol. 72, No. 2, April, (2000), p. 418.

64. J. D. Jackson, *Classical Electrodynamics*, Second Edition, John Wiley & Sons, New York,

(1975), pp. 236-240, 601-608, 786-790.

65. J. D. Jackson, *Classical Electrodynamics*, Second Edition, John Wiley & Sons, New York, (1975), p. 178.

66. P. J. Mohr, B. N. Taylor, "CODATA recommended values of the fundamental physical constants: 1998", Reviews of Modern Physics, Vol. 72, No. 2, April, (2000), pp. 418-419.

67. Patz, S., Cardiovasc Interven Radiol, (1986), 8:25, pp. 225-237.

68. W. Liu, M. G. Boshier, S. Dhawan, O. van Dyck, P. Egan, X. Fei, M. Grosse Perdekamp, V. W. Hughes, M. Janousch, K. Jungmann, D. Kawall, F. G. Mariam, C. Pillai, R. Prigl, G. zu Putlitz, I. Reinhard, W. Schwarz, P. A. Thompson, K. A. Woodle, "High Precision measurements of the ground state hyperfine structure interval of muonium and the muon magnetic moment", Phys. Rev. Lett., Vol. 82, No. 4, (1999), pp. 711-714.

69. P. J. Mohr, B. N. Taylor, "CODATA recommended values of the fundamental physical constants: 1998", Reviews of Modern Physics, Vol. 72, No. 2, April, (2000), pp. 448-453.

70. P. J. Mohr, B. N. Taylor, "CODATA recommended values of the fundamental physical constants: 2002", in press, http://physics.nist.gov/constants.

71. M. W. Ritter, P. O. Egan, V. W. Hughes, K. A. Woodle, "Precision determination of the hyperfine structure interval in the ground state of positronium. V", Phys. Rev. A, Vol. 30, No. 3, (1984), pp. 1331-1338.

72. J. D. Jackson, *Classical Electrodynamics*, Second Edition, John Wiley & Sons, New York, (1975), p. 9.

Table I. Relativistically corrected ionization energies for some one-electron atoms.

One e Atom	Z	γ^* a	Theoretical Ionization Energies (eV) b	Experimental Ionization Energies (eV) c	Relative Difference between Experimental and Calculated d
H	1	1.000007	13.59838	13.59844	0.00000
He^{+}	2	1.000027	54.40941	54.41778	0.00015
Li^{2+}	3	1.000061	122.43642	122.45429	0.00015
Be^{3+}	4	1.000109	217.68510	217.71865	0.00015
B^{4+}	5	1.000172	340.16367	340.2258	0.00018
C^{5+}	6	1.000251	489.88324	489.99334	0.00022
N^{6+}	7	1.000347	666.85813	667.046	0.00028
O^{7+}	8	1.000461	871.10635	871.4101	0.00035
F^{8+}	9	1.000595	1102.65013	1103.1176	0.00042
Ne^{9+}	10	1.000751	1361.51654	1362.1995	0.00050
Na^{10+}	11	1.000930	1647.73821	1648.702	0.00058
Mg^{11+}	12	1.001135	1961.35405	1962.665	0.00067
Al^{12+}	13	1.001368	2302.41017	2304.141	0.00075
Si^{13+}	14	1.001631	2670.96078	2673.182	0.00083
P^{14+}	15	1.001927	3067.06918	3069.842	0.00090
S^{15+}	16	1.002260	3490.80890	3494.1892	0.00097
Cl^{16+}	17	1.002631	3942.26481	3946.296	0.00102
Ar^{17+}	18	1.003045	4421.53438	4426.2296	0.00106
K^{18+}	19	1.003505	4928.72898	4934.046	0.00108

Ca^{19+}	20	1.004014	5463.97524	5469.864	0.00108
Sc^{20+}	21	1.004577	6027.41657	6033.712	0.00104
Ti^{21+}	22	1.005197	6619.21462	6625.82	0.00100
V^{22+}	23	1.005879	7239.55091	7246.12	0.00091
Cr^{23+}	24	1.006626	7888.62855	7894.81	0.00078
Mn^{24+}	25	1.007444	8566.67392	8571.94	0.00061
Fe^{25+}	26	1.008338	9273.93857	9277.69	0.00040
Co^{26+}	27	1.009311	10010.70111	10012.12	0.00014
Ni^{27+}	28	1.010370	10777.26918	10775.4	-0.00017
Cu^{28+}	29	1.011520	11573.98161	11567.617	-0.00055

[a] Eq. (1.250) of Ref. [7] (follows Eqs. (6), (16), and (60)).

[b] Eq. (1.251) of Ref. [7] (Eq. (64) times γ^*).

[c] From theoretical calculations, interpolation of H isoelectronic and Rydberg series, and experimental data [51-52].

[d] (Experimental-theoretical)/experimental.

Figure Captions

Figure 1. The orbitsphere is a two dimensional spherical shell of zero thickness with the Bohr radius of the hydrogen atom, $r = a_H$.

Figure 2A-C. The current pattern of the orbitsphere from the perspective of looking along the z-axis, x-axis, and y-axis, respectively. The current and charge density are confined to two dimensions at $r_n = nr_1$. The corresponding charge density function is uniform.

Figure 3. The orbital function modulates the constant (spin) function (shown for t = 0; three-dimensional view).

Figure 4. The current on the great circle in the y'z'-plane moves counter clockwise and the current on the great circle in the x'z'-plane moves clockwise. The xyz-system is the laboratory frame, and the orthogonal-current-loop basis set is rigid with respect to the x'y'z'-system that rotates about the $\left(\mathbf{i}_x, \mathbf{i}_y, 0\mathbf{i}_z\right)$-axis by π radians to generate the elements of the first component of the orbitsphere-cvf. The angular momentum of the orthogonal great circle current loops in the x'y'-plane that is evenly distributed over the surface is $\frac{\hbar}{2\sqrt{2}}$.

Figure 5. The current pattern of the orbitsphere-cvf component of STEP ONE shown with 6 degree increments of θ from the perspective of looking along the z-axis. The yz-plane great circle current loop that served as a basis element that was initially in the yz-plane is shown as red.

Figure 6. The current pattern of the orbitsphere-cvf component of STEP ONE shown with 6 degree increments of θ from the perspective of looking along the z-axis. The great circle current loop that served as a basis element that was initially in the xz-plane is shown as red.

Figure 7. The current on the great circle in the plane that bisects the x'y'-quadrant and is parallel to the z'-axis moves clockwise, and the current on the great circle in the x'y'-plane moves counter clockwise. Rotation of the great circles about the $\left(-\frac{1}{\sqrt{2}}\mathbf{i}_x,\frac{1}{\sqrt{2}}\mathbf{i}_y,\mathbf{i}_z\right)$-axis by π radians generates the elements of the second component of the orbitsphere-cvf. The angular momentum of the orthogonal great circle current loops in the plane along the $\left(-\frac{1}{\sqrt{2}}\mathbf{i}_x,\frac{1}{\sqrt{2}}\mathbf{i}_y,\mathbf{i}_z\right)$- and z-axes is $\frac{\hbar}{2\sqrt{2}}$ corresponding to each of the z and -xy-components of magnitude $\frac{\hbar}{4}$.

Figure 8. The current pattern of the orbitsphere-cvf component of STEP TWO shown with 6 degree increments of θ from the perspective of looking along the z-axis. The great circle current loop that served as a basis element that was initially in the plane that bisects the xy-quadrant and was parallel to the z-axis is shown as red.

Figure 9. The current pattern of the orbitsphere-cvf component of STEP TWO shown with 6 degree increments of θ from the perspective of looking along the z-axis. The great circle current loop that served as a basis element that was initially in the xy-plane is shown as red.

Figure 10. The normalized radius as a function of the velocity due to relativistic contraction (Eq. (16)).

Figure 11. The magnetic field of an electron orbitsphere (z-axis defined as the vertical axis).

Figure 12. Broadening of the spectral line due to the rise-time and shifting of the spectral line due to the radiative reaction. The resonant line shape has width Γ. The level shift is $\Delta\omega$.

Fig. 1.

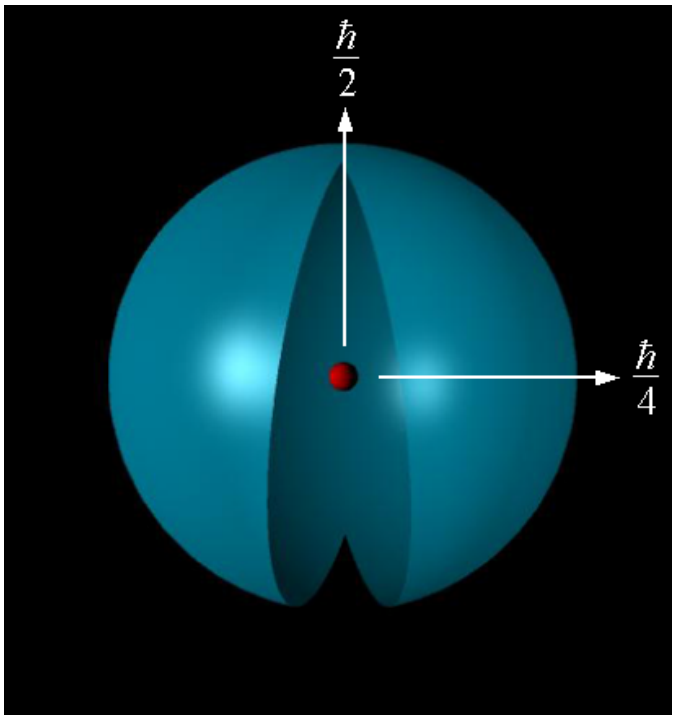

Fig. 2

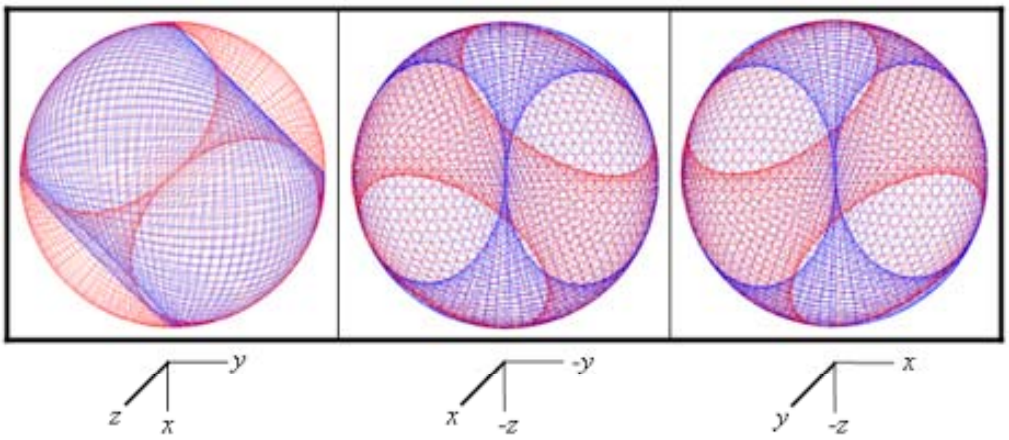

Fig. 3

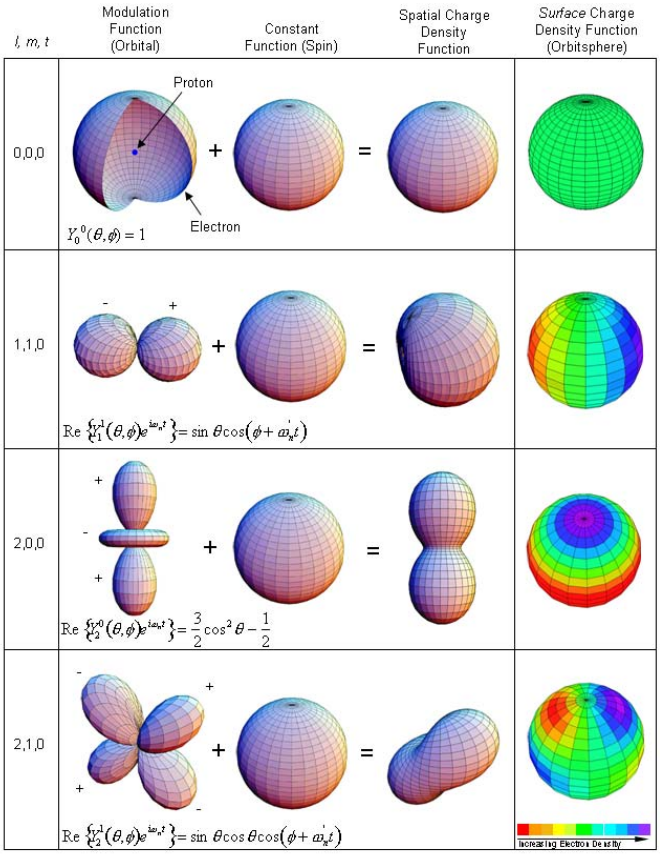
l, m, t
Modulation Function (Orbital)
Constant Function (Spin)
Spatial Charge Density Function
Surface Charge Density Function (Orbitsphere)
0,0,0
Proton
Electron
$Y_0^0(\theta,\phi)=1$
1,1,0
$\mathrm{Re}\left\{Y_1^1(\theta,\phi)e^{i\omega_n t}\right\}=\sin\theta\cos\left(\phi+\omega_n^1 t\right)$
2,0,0
$\mathrm{Re}\left\{Y_2^0(\theta,\phi)e^{i\omega_n t}\right\}=\frac{3}{2}\cos^2\theta-\frac{1}{2}$
2,1,0
$\mathrm{Re}\left\{Y_2^1(\theta,\phi)e^{i\omega_n t}\right\}=\sin\theta\cos\theta\cos\left(\phi+\omega_n^1 t\right)$
Increasing Electron Density

Fig. 4

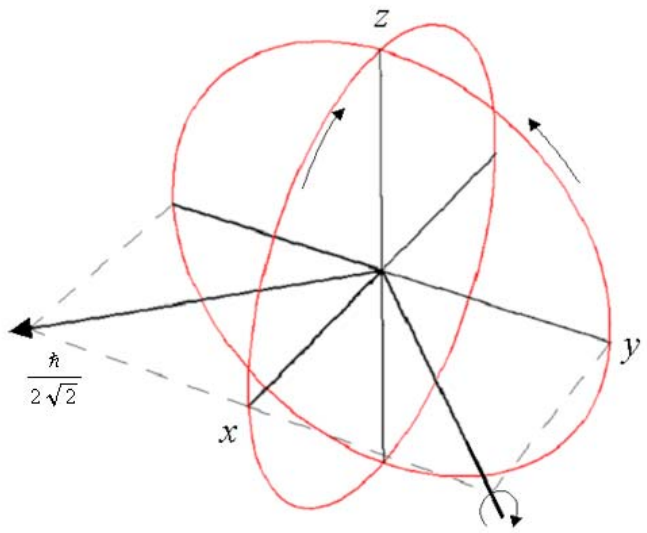

Fig. 5

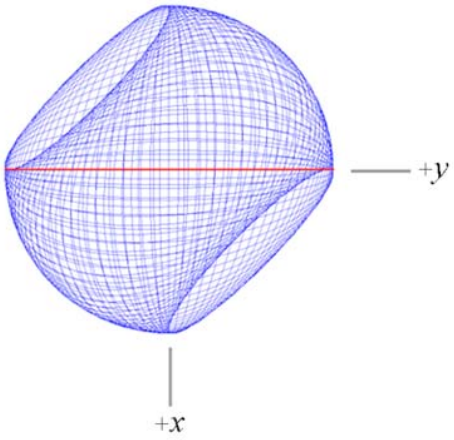

Fig. 6

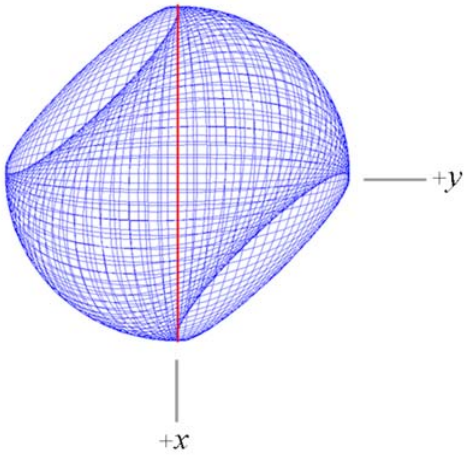

Fig. 7

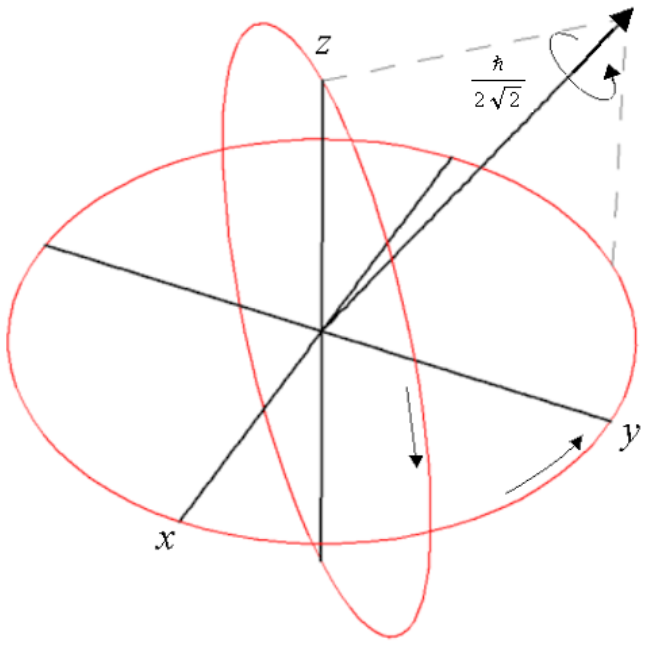

Fig. 8

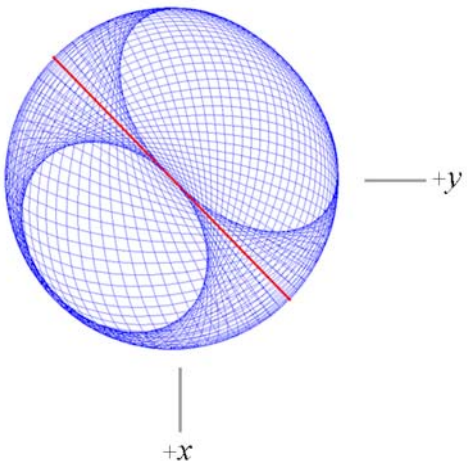

Fig. 9

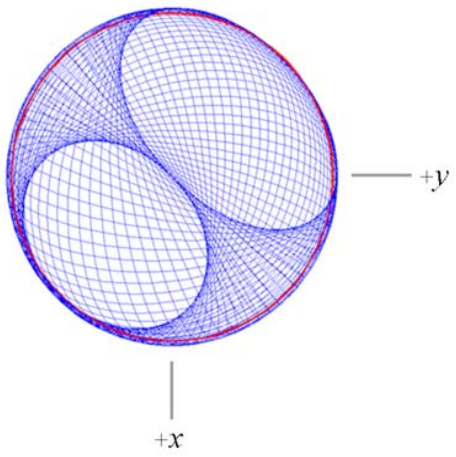

Fig. 10

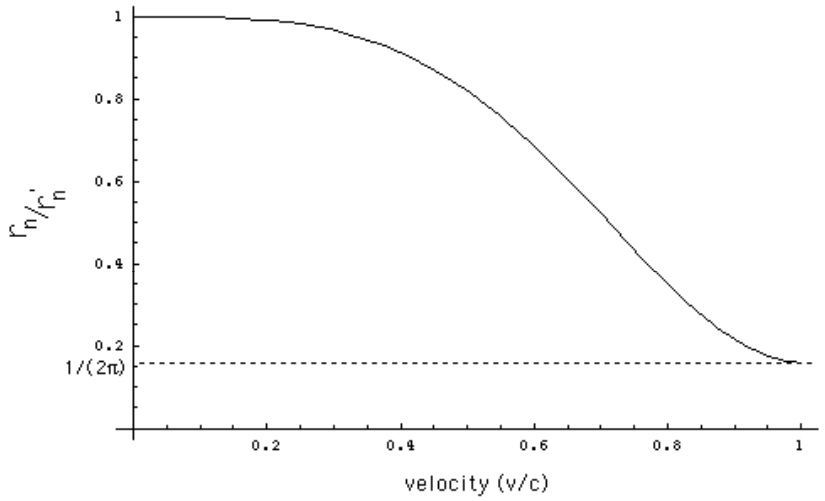

Fig. 11

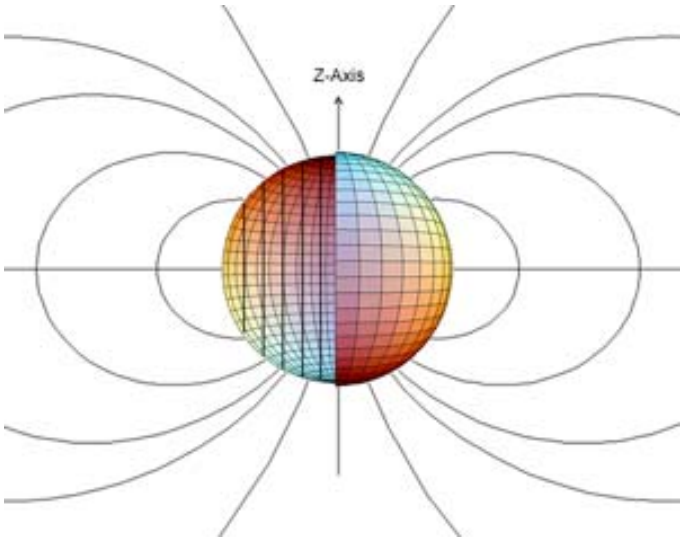

Fig. 12